# Generalized Sheet Transition Conditions for a Metascreen—A Fishnet Metasurface

Christopher L. Holloway, *Fellow, IEEE*, and Edward F. Kuester, *Life Fellow, IEEE*

***Abstract*— We used a multiple-scale homogenization method to derive generalized sheet transition conditions (GSTCs) for electromagnetic fields at the surface of a metascreen—a metasurface with a "fishnet" structure. These surfaces are characterized by periodically spaced arbitrary-shaped apertures in an otherwise relatively impenetrable surface. The parameters in these GSTCs are interpreted as effective surface susceptibilities and surface porosities, which are related to the geometry of the apertures that constitute the metascreen. We emphasize the subtle but important difference between the GSTCs required for metascreens and those required for metafilms [a metasurface with a "cermet" structure, i.e., an array of isolated (nontouching) scatterers]. Finally, we demonstrate the validity of the surface parameters derived here by comparing results for metascreens composed of either circular or square apertures with those of other approaches.**

***Index Terms*— Boundary conditions (BCs), generalized sheet transition conditions (GSTCs), metafilms, metagratings, metamaterials, metascreens, metasurfaces, multiple-scale homogenization, surface porosities, surface susceptibilities.**

## I. Introduction

IN RECENT years, there has been a great deal of interest in electromagnetic metamaterials [1]–[7]—novel synthetic materials engineered to achieve desirable/unique properties not normally found in nature. Metamaterials are often engineered by positioning scatterers throughout a 3-D region of space in order to achieve some desirable bulk behavior of the material (typically a behavior not normally occurring). This concept can be extended by placing scatterers (or apertures) in a 2-D arrangement at a surface or an interface. This surface version of a metamaterial is called a metasurface and includes metafilms and metascreens as special cases [8], [9].

Metasurfaces are an attractive alternative to 3-D metamaterials because of their simplicity and relative ease of fabrication. While, in general, a metasurface can be either a periodic or nonperiodic surface, in this paper, we consider only periodic structures. We will thus understand a metasurface to be a 2-D structure whose thickness and periodicity are small compared with a wavelength in the surrounding media. Metasurfaces should not be confused with classical frequency-selective surfaces [10], [11]; the important distinction between the two is discussed in [8]. As discussed in [12], we can identify two important subclasses (metafilms and metascreens) within this general designation of metasurfaces. These two subclasses are distinguished by the topology of the metasurface. Metafilms (as coined in [13]) are metasurfaces that have a "cermet" topology, which refers to an array of isolated (nontouching) scatterers [see Fig. 1(a)]. Metascreens are metasurfaces with a "fishnet" structure [see Fig. 1(b)], which are characterized by periodically spaced apertures in an otherwise relatively impenetrable surface. There are other types of metastructures that lie somewhere between a metafilm and a metascreen. For example, a grating of parallel coated wires (a metagrating) behaves like a metafilm to electric fields perpendicular to the wire axes and like a metascreen for electric fields parallel to the wire axis [14]. In this paper, we discuss the behavior of metascreens. Note that the thickness $h$ of the screen in which the apertures of the metascreen are located is not necessarily zero (or even small compared with the lattice constants). The apertures are arbitrarily shaped, and their dimensions are required to be small only in comparison with a wavelength in the surrounding medium, i.e., the thickness and aperture sizes are electrically small. The important distinction between the behavior of a metafilm and that of a metascreen or metagrating is that the isolated scatterers in a metafilm imply that currents flowing along the surface are small (of the order of the lattice constant divided by the wavelength). As will be discussed in the following, metascreens and metagratings may have essentially nonzero currents along their surface even in the limit of vanishing lattice constant, and as a result, boundary conditions (BCs) used for metafilms are not appropriate for metascreens or metagratings.

While metafilms have been investigated extensively in the past [8], [9], [12]–[17], metascreens have received less attention, which is mainly due to not having efficient ways of analyzing them. In this paper, we derive the required BCs needed to fully characterize a metascreen. These BCs are called generalized sheet transition conditions (GSTCs) and will provide a framework for the efficient modeling and synthesis of metascreens, much in the same way that GSTCs have been very useful in the modeling and design of metafilms, because repeated full-wave simulations are not required in the initial stages of synthesis. However, as we will see, the required GSTCs needed for a metascreen are fundamentally different from those required for a metafilm.

Given a generic metasurface (either a metafilm, a metascreen, or a metagrating), one could use any of

Manuscript received October 9, 2017; revised February 14, 2018; accepted February 16, 2018. Date of publication February 27, 2018; date of current version May 3, 2018. *(Corresponding author: Christopher L. Holloway.)*

C. L. Holloway is with Boulder Laboratories, Electromagnetics Division, U.S. Department of Commerce, National Institute of Standards and Technology, Boulder, CO 80305 USA (e-mail: holloway@boulder.nist.gov).

E. F. Kuester is with the Department of Electrical, Computer and Energy Engineering, University of Colorado at Boulder, Boulder, CO 80309 USA.

Color versions of one or more of the figures in this paper are available online at http://ieeexplore.ieee.org.

Digital Object Identifier 10.1109/TAP.2018.2809620

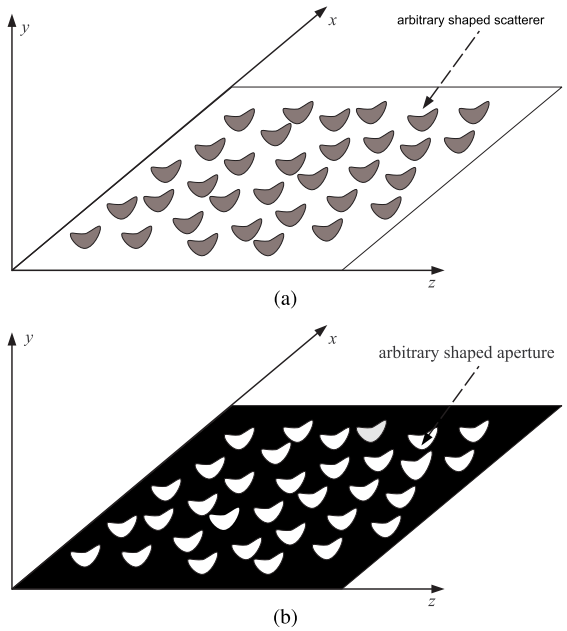


Fig. 1. Illustration of types of metasurfaces. (a) Metafilm which consists of arbitrarily shaped scatterers placed on the $xz$-plane. (b) Metascreen which consists of arbitrarily shaped apertures in a conducting screen located in the $xz$-plane.

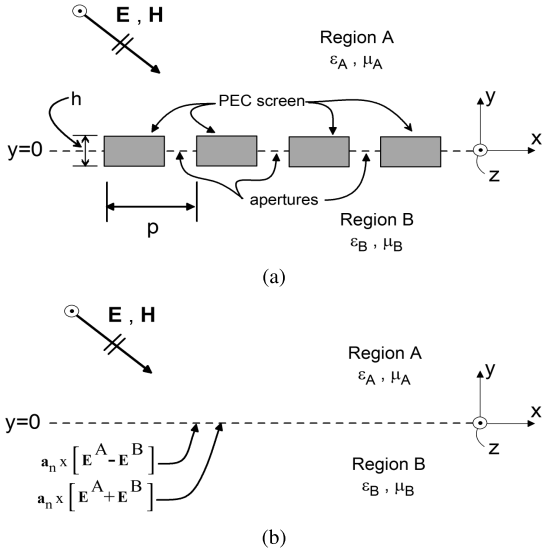


Fig. 2. (a) Metascreen (array of apertures in conducting screen) and (b) reference plane at which the GSTCs are applied.

the commercially available software tools for electromagnetic simulation to analyze the interaction of an electromagnetic field with that metasurface. However, it has been shown throughout the literature that GSTCs for metafilms have been beneficial in more easily providing physical insight into the analysis or synthesis of metafilms than the purely numerical approach. Such GSTCs for metascreens have not been available in the past. Those developed here for the metascreen will allow us to efficiently analyze the interesting behaviors of metascreens in order to obtain insight into the surface parameters and their effects on the metascreen behavior, which is beneficial for various applications. In particular, the GSTCs will provide clear guidelines on how the surface parameters should be chosen to achieve some desired behavior, inasmuch as such insight cannot be obtained as easily from numerical approaches.

We start with an explanation of the general features of effective BCs (EBCs) required to describe the interaction of electromagnetic fields with the metascreen of Fig. 1(b). A formal proof is not given here; however, we will present arguments that indicate the type of BCs that are required to obtain unique solutions for the fields at the interface or the surface of a metascreen. We start by noting that the desired type of EBC will allow the metascreen to be replaced by the interface, as shown in Fig. 2. Furthermore, we want the interaction of the electric ($E$) and magnetic ($H$) fields on either side of the metascreen to be taken care of through some type of GSTC applied at that interface. In this type of EBC, all the information about the metascreen (geometry: shape, size, material properties, and so on) is incorporated into the parameters that appear explicitly in the GSTC.

In previous work, it has been shown that such GSTCs are the most appropriate way to model metafilms [13], [15]–[17]. The form of GSTCs used for the metafilm is basically a set of BCs for the jumps in both tangential $E$- and $H$-fields at the surface of the metafilm. As it turns out, because of the distinctive properties of a metascreen, GSTCs can still be used, but they must take a different form. The reason for this different form is as follows. For a two-region problem, one needs at least two EBCs for constraining the tangential $E$- and/or $H$-fields. The issue with a metascreen is that there is the possibility of having tangential surface currents (flowing on the surface of the screen along the $z$- and $x$-direction) that do not vanish as the lattice constant of the metascreen approaches zero. Typically, these currents would only be known once the tangential components of the $H$-field are known. An example of this is the case of an electromagnetic field at the surface of a perfect electric conductor (PEC). For a PEC, only the BC for the tangential $E$-field at the PEC (i.e., $\mathbf{E}_t = 0$ on the PEC) is used in solving boundary problems for the field. The BC for the tangential $H$-field at the PEC is not used at this point but is instead related to the surface current flowing on the PEC; this current is only known once the $H$-field has been determined. It is useful, therefore, to classify EBCs either as *essential* for the solution of an electromagnetic boundary problem, or applicable only *a posteriori* when quantities, such as surface current or charge density, are to be computed from the fields. For a metascreen, any EBC for the tangential $H$-field is an *a posteriori* BC and can only be used once the fields have been solved. Thus, the required *essential* BCs for metascreen should constrain only tangential $E$ and not tangential $H$ and could be expressed as conditions on the jump in the tangential $E$-field and on the sum (twice the average) of the tangential $E$-fields, i.e.,

$$\begin{bmatrix} E_x^A - E_x^B \end{bmatrix}_{y=0} \quad \begin{bmatrix} E_z^A - E_z^B \end{bmatrix}_{y=0}$$
$$\begin{bmatrix} E_x^A + E_x^B \end{bmatrix}_{y=0} \quad \begin{bmatrix} E_z^A + E_z^B \end{bmatrix}_{y=0} \tag{1}$$

where the superscripts $A$ and $B$ correspond to the regions above and below the reference plane of the metascreen,

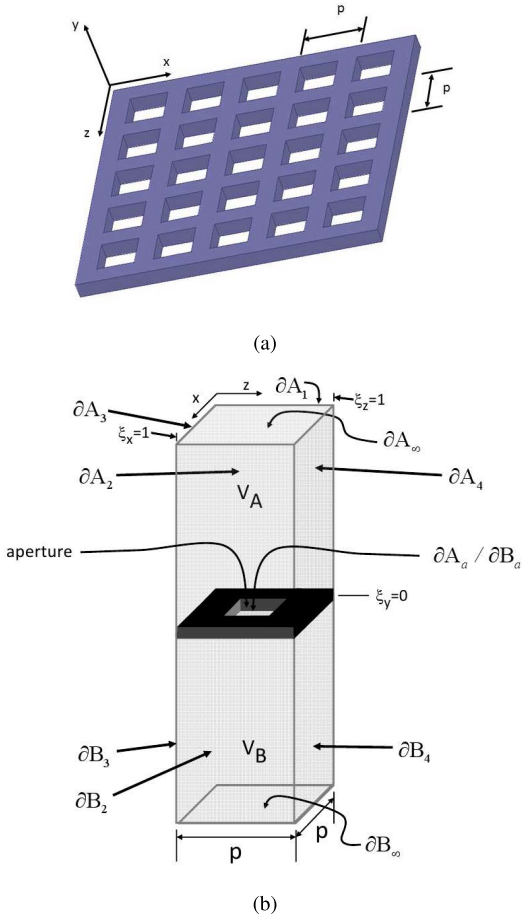


Fig. 3. (a) Periodic metascreen. (b) Period cell.

respectively. These types of GSTCs (on both the jump in, and the average of, the $E$-field at the interface) have also appeared in the analysis of a wire grating (or metagrating) [14].

In this paper, we present a systematic multiple-scale homogenization approach to fully characterize the field interaction at the surface of the periodic metascreen, as shown in Fig. 3(a). With this method, we derive equivalent (or "averaged") BCs for the metascreen. Due to the geometry of the metascreen, the fields at the interface have both a behavior localized near the apertures and a global (or average) behavior. The localized field behavior varies on a length scale of the order of the spacing of the apertures, while the global field behavior varies on a scale of the order of a wavelength. This local field behavior can be separated from that of the average field (with multiple-scale homogenization [14], [17]–[25]). This technique allows for the fields to be expressed as a product of two functions, one carrying the fine structure and the other the global behavior. It is, therefore, possible to derive GSTCs for the average or effective field. The electromagnetic scattering from a metascreen can be approximated by applying the GSTCs at the interface of the two media on either side of the metascreen (as shown in Fig. 2); thus, the GSTCs are all that is required to determine macroscopic scattering and reflection from the metascreen.

## II. Derivation of GSTCs and Asymptotic Expansions

Some of the derivation of the desired GSTCs are analogous to that used in [14], [17], and [23]–[25], and thus, we will not show some of the details when they can be found in these citations. In this section, we first expand the fields in powers of $k_0 p$ (where $p$ is the period of the array, $k_0 = \omega\sqrt{\mu_0\epsilon_0}$ is the free-space wavenumber, and $\omega$ is the angular frequency corresponding to an assumed $\exp(j\omega t)$ time dependence). We next determine the BCs for the various components of the field. Finally, the solution for this set of boundary-value problems will lead to the desired GSTCs for the metascreen.

### A. Asymptotic Expansion of Maxwell's Equations

Let an electromagnetic field be incident onto the array of apertures, as shown in Figs. 2 and 3. This array of apertures is periodic in the $xz$-plane, and we assume that the two media on either side of the metascreen are different. The analysis to be presented here is valid for any arbitrarily shaped aperture. In addition, the surfaces of the PEC screen will, for simplicity, be depicted as planar, with vertical aperture sides; this too is not a crucial restriction, and the screen thickness can vary with $x$ and $z$ so long as it remains small compared with a wavelength.

In this analysis, we assume that the two media are homogeneous, and that the screen containing the apertures is a PEC. However, one can show that if we assume the plane is composed of a more general material (e.g., a magnetodielectric medium with large $\epsilon$ or $\mu$), the form of the GSTCs is the same, and the only difference is in the surface parameters that characterize the metascreen. Thus, by assuming a PEC screen, we can easily present the framework of the analysis, knowing that the final form of the GSTC will be the same for a more general magneto-dielectric screen. In the case of a highly conducting screen or one where resonances are present, the technique of "stiff" homogenization must be used [23], [26]–[29].

The underlying assumption is that the period $p$ of the array of apertures is small. This results in two spatial length scales: one corresponding to the source or incident wave (the free-space wavelength $\lambda_0$) and the other corresponding to the microstructure of the periodic array of apertures ($p$). These two spatial length scales cause the fields to have a multiple-scale type variation that is associated with the macroscopic and microscopic structures of the problem. Similar to [14], [17], and [23]–[25], Maxwell's equations are expressed as

$$\nabla\times\mathbf{E}^{(A,B)\,T} = -j\omega\mathbf{B}^{(A,B)\,T} \;:\; \nabla\times\mathbf{H}^{(A,B)\,T} = j\omega\mathbf{D}^{(A,B)\,T} \tag{2}$$

with

$$\mathbf{D}^{(A,B)\,T} = \epsilon_0\epsilon_r\mathbf{E}^{(A,B)\,T} \;:\; \mathbf{B}^{(A,B)\,T} = \mu_0\mu_r\mathbf{H}^{(A,B)\,T} \tag{3}$$

where superscript $T$ corresponds to the total fields (i.e., containing both the localized and global behaviors), while $\mu_r$ is the relative permeability and $\epsilon_r$ is the relative permittivity at

a given location. The superscripts $A$ and $B$ correspond to the regions above and below the reference plane (located at $y = 0$) of the metascreen, respectively.

Following [17] and [23]–[25], we use a multiple-scale representation for the fields:

$$\mathbf{E}^T(\mathbf{r}, \boldsymbol{\xi}) = \mathbf{E}^T\left(\frac{\hat{\mathbf{r}}}{k_0}, \boldsymbol{\xi}\right). \tag{4}$$

Similar expressions are used for the other fields. Here, $\mathbf{r}$ is defined as the *slow* spatial variable, and $\hat{\mathbf{r}}$ is defined as a dimensionless *slow* variable given by

$$\mathbf{r} = x\mathbf{a}_x + y\mathbf{a}_y + z\mathbf{a}_z \quad \text{and } \hat{\mathbf{r}} = k_0\mathbf{r} \tag{5}$$

while the scaled dimensionless variable $\boldsymbol{\xi}$ is called the *fast* variable, defined as

$$\boldsymbol{\xi} = \frac{\mathbf{r}}{p} = \mathbf{a}_x\frac{x}{p} + \mathbf{a}_y\frac{y}{p} + \mathbf{a}_z\frac{z}{p} = \mathbf{a}_x\xi_x + \mathbf{a}_y\xi_y + \mathbf{a}_z\xi_z \tag{6}$$

where $p$ is the period of the apertures that constitute the metascreen. This period $p$ is assumed to be small compared with all other macroscopic lengths in the problem. Note that the slow variable $\hat{\mathbf{r}}$ has significant changes over distances on the order of a wavelength, while the fast variable has changes over much smaller distances, i.e., on the order of $p$.

Close to the metascreen, we should expect microscopic variations of the fields with $\boldsymbol{\xi}$. However, once away from the metascreen, this behavior should die out. This allows for a boundary-layer field representation for the localized field terms, and as such the total fields can be expressed as

$$\mathbf{E}^{(A,B)\ T} = \mathbf{E}^{A,B}(\hat{\mathbf{r}}) + \mathbf{e}^{\mathbf{A},\mathbf{B}}(\hat{\mathbf{r}}, \boldsymbol{\xi}). \tag{7}$$

We can write a similar expression for $\mathbf{H}^{(A,B)\ T}$. Here, we denote $\mathbf{E}$ and $\mathbf{H}$ as "nonboundary-layer" or "macroscopic" fields, which are referred to as the effective fields in this paper. The quantities $\mathbf{e}$ and $\mathbf{h}$ are called the boundary-layer fields. These fields are periodic in $\xi_x$ and $\xi_z$ (because of the periodicity of the array of apertures), but decay exponentially in $\xi_y$

$$\mathbf{e}^{\mathbf{A},\mathbf{B}} \quad \text{and } \mathbf{h}^{\mathbf{A},\mathbf{B}} = O(e^{-(\text{const})|\xi_y|}) \quad \text{as } |\xi_y| \to \infty. \tag{8}$$

These boundary-layer fields are functions of both the *slow* and *fast* variables. As shown in [14], [17], and [23]–[25], for other periodic structures, the boundary-layer fields are functions of just five variables: two slow variables $(\hat{x}, \hat{z})$ at the interface (which we express succinctly by the position vector $\hat{\mathbf{r}}_o = \mathbf{a}_x\hat{x} + \mathbf{a}_z\hat{z} \equiv k_0\mathbf{r}_o$) and three fast variables $(\boldsymbol{\xi})$

$$\mathbf{e}(\hat{\mathbf{r}}_o, \boldsymbol{\xi}). \tag{9}$$

To account for the two length scales in this multiple-scale analysis, the nabla operator is expressed in terms of the scaled variables [24]

$$\nabla \to k_0\nabla_{\hat{r}} + \frac{1}{p}\nabla_\xi \tag{10}$$

where

$$\nabla_{\hat{r}} = \mathbf{a}_x\frac{\partial}{\partial\hat{x}} + \mathbf{a}_y\frac{\partial}{\partial\hat{y}} + \mathbf{a}_z\frac{\partial}{\partial\hat{z}} \tag{11}$$

and

$$\nabla_\xi = \mathbf{a}_x\frac{\partial}{\partial\xi_x} + \mathbf{a}_y\frac{\partial}{\partial\xi_y} + \mathbf{a}_z\frac{\partial}{\partial\xi_z}. \tag{12}$$

With this, the curl equations are

$$\begin{aligned} \nabla_{\hat{r}} \times \mathbf{E} + \nabla_{\hat{r}} \times \mathbf{e} + \frac{1}{\nu}\nabla_\xi \times \mathbf{e} &= -jc(\mathbf{B} + \mathbf{b}) \\ \nabla_{\hat{r}} \times \mathbf{H} + \nabla_{\hat{r}} \times \mathbf{h} + \frac{1}{\nu}\nabla_\xi \times \mathbf{h} &= jc(\mathbf{D} + \mathbf{d}) \end{aligned} \tag{13}$$

where $\nu$ is a small dimensionless parameter given by

$$\nu = k_0\, p$$

and $c$ is the speed of light *in vacuo*.

The relative permeability $(\mu_r)$ and relative permittivity $(\epsilon_r)$ of the two media are expressed by

$$\epsilon_r = \left\{ \begin{matrix} \epsilon_A\ (y > 0) \\ \epsilon_B\ (y < 0) \end{matrix} \right\}, \quad \mu_r = \left\{ \begin{matrix} \mu_A\ (y > 0) \\ \mu_B\ (y < 0) \end{matrix} \right\} \tag{14}$$

where $\epsilon_{A,B}$ and $\mu_{A,B}$ are the background relative permittivity and permeability of the regions A and B. These material properties may be discontinuous at the plane $\xi_y = 0$ (i.e., $y = 0$). This reference plane ($y = 0$) is the division between the two background materials and, in our structure, corresponds to the center plane of the metal aperture (see Fig. 2). This reference plane can be chosen at any convenient location in the boundary layer, even below or above the metascreen. The $y = 0$ plane can be thought of as located at the "center" of the apertures composing the metascreen, but this restriction is not necessary, and a change in the location of this reference plane would cause only changes in the coefficients (i.e., the surface parameters) appearing in the GSTCs. This would result in shifts in the phase of, say, the plane-wave reflection coefficient obtained from it. The matter of reference-plane location is discussed in [24], [30], and [31]. Using the above-mentioned description of $\epsilon_r$ and $\mu_r$, the constitutive equations (3) are

$$\begin{aligned} \mathbf{D} &= \epsilon_0\epsilon_r\mathbf{E}, \quad \mathbf{B} = \mu_0\mu_r\mathbf{H} \\ \mathbf{d} &= \epsilon_0\epsilon_r\mathbf{e}, \quad \mathbf{b} = \mu_0\mu_r\mathbf{h}. \end{aligned} \tag{15}$$

Recall that the boundary-layer fields appearing in (13) vanish by (8) as $|\xi_y| \to \infty$. As a result, the fields away from the metascreen obey the following macroscopic Maxwell equations:

$$\nabla_{\hat{r}} \times \mathbf{E} = -jc\mathbf{B} \quad \text{and } \nabla_{\hat{r}} \times \mathbf{H} = jc\mathbf{D}. \tag{16}$$

However, because the effective fields are independent of $\boldsymbol{\xi}$, (16) is true for all $\hat{\mathbf{r}}$ (i.e., even up to the $y = 0$ plane of the metascreen). Eliminating the effective fields from (13) gives

$$\begin{aligned} \nabla_{\hat{r}} \times \mathbf{e} + \frac{1}{\nu}\nabla_\xi \times \mathbf{e} &= -jc\mathbf{b} \\ \nabla_{\hat{r}} \times \mathbf{h} + \frac{1}{\nu}\nabla_\xi \times \mathbf{h} &= jc\mathbf{d}. \end{aligned} \tag{17}$$

We are only interested in the situation when the period is small compared with a wavelength, which corresponds

to $\nu \ll 1$. Thus, we expand the fields in powers of the small dimensionless parameter $\nu$

$$\begin{aligned}\mathbf{E} &\sim \mathbf{E}^0(\mathbf{r}) + \nu\mathbf{E}^1(\mathbf{r}) + O(\nu^2)\\ \mathbf{e} &\sim \mathbf{e}^0(\mathbf{r}_o, \boldsymbol{\xi}) + \nu\mathbf{e}^1(\mathbf{r}_o, \boldsymbol{\xi}) + O(\nu^2).\end{aligned} \tag{18}$$

A similar set of expressions is obtained for each of the other fields. The lowest order fields ($\mathbf{E}^0$, $\mathbf{H}^0$, and so on) will include any incident fields which may be present, as well as the zeroth-order scattered field.

If we substitute the first line of (18) into (16) and group like powers of $\nu$, we find that each order of effective fields $\mathbf{E}^m$ and $\mathbf{H}^m$ ($m = 0, 1, \ldots$) satisfies the macroscopic Maxwell's equations (16). On the other hand, if we substitute the second line of (18) into the second line of (15) and group like powers of $\nu$ we obtain

$$\nu^0 : \mathbf{b}^0 = \mu_0\mu_r\mathbf{h}^0 \quad \text{and } \mathbf{d}^0 = \epsilon_0\epsilon_r\mathbf{e}^0 \tag{19}$$

$$\nu^1 : \mathbf{b}^1 = \mu_0\mu_r\mathbf{h}^1 \quad \text{and } \mathbf{d}^1 = \epsilon_0\epsilon_r\mathbf{e}^1 \tag{20}$$

and so on for higher powers. We also find that the boundary-layer fields satisfy the following:

$$\begin{aligned}\nu^{-1} : \nabla_\xi \times \mathbf{e}^0 &= 0\\ \nabla_\xi \times \mathbf{h}^0 &= 0\end{aligned} \tag{21}$$

$$\begin{aligned}\nu^0 : \nabla_\xi \times \mathbf{e}^1 &= -jc\mathbf{b}^0 - \nabla_{\hat{r}} \times \mathbf{e}^0\\ \nabla_\xi \times \mathbf{h}^1 &= jc\mathbf{d}^0 - \nabla_{\hat{r}} \times \mathbf{h}^0\end{aligned} \tag{22}$$

$$\begin{aligned}\nu^1 : \nabla_\xi \times \mathbf{e}^2 &= -jc\mathbf{b}^1 - \nabla_{\hat{r}} \times \mathbf{e}^1\\ \nabla_\xi \times \mathbf{h}^2 &= jc\mathbf{d}^1 - \nabla_{\hat{r}} \times \mathbf{h}^1\end{aligned} \tag{23}$$

and so on for high powers. Finally, taking the fast divergence $\nabla_\xi\cdot$ of (22) gives

$$\nabla_\xi \cdot \mathbf{b}^0 = 0 \quad \text{and } \nabla_\xi \cdot \mathbf{d}^0 = 0. \tag{24}$$

These results show that $\mathbf{e}^0$ and $\mathbf{h}^0$ are 2-D static fields [as seen by (21) and (24)]. They also are periodic in $\xi_x$ and $\xi_z$, and decay exponentially as $|\xi_y| \to \infty$.

Taking the fast divergence $\nabla_\xi\cdot$ of (23) and using (22) give

$$\nabla_\xi \cdot \mathbf{b}^1 = -\nabla_{\hat{r}} \cdot \mathbf{b}^0 \quad \text{and } \nabla_\xi \cdot \mathbf{d}^1 = -\nabla_{\hat{r}} \cdot \mathbf{d}^0 \tag{25}$$

which, together with (22), gives the complete set of differential equations needed to determine the first-order boundary-layer fields.

In summary, as we would expect, this multiple-scale representation shows that the effective fields obey the macroscopic Maxwell's equation (16). By contrast, the boundary-layer fields at the zeroth order obey the static field equations (21) and (24) and obey (22) and (25) at the first order.

To complete the mathematical description of the problem, BCs must be specified. This will allow the effective fields at $y = 0$ to be related to the boundary-layer fields at the metascreen interface. Section III-C shows that to first order, the required BCs for the effective fields depend only on the zeroth-order boundary-layer fields and not on the higher order boundary-layer fields. Therefore, the desired BCs for the effective fields can be obtained once these zeroth-order boundary-layer fields are determined.

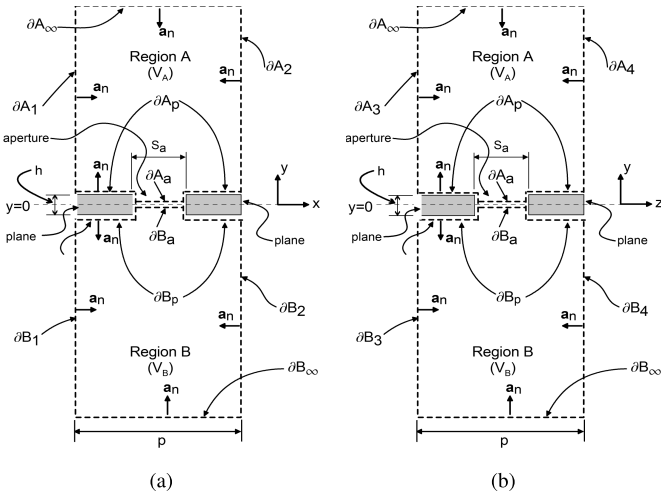


Fig. 4. Period cell with various boundaries defined: (a) $yx$-plane and (b) $yz$-plane. The interior volume of the screen is defined by $V_s$, which is divided into the portions $V_{sA}$ and $V_{sB}$ lying above and below $\xi_y = 0$, respectively.

### B. Boundary Conditions on the Screen and at the Interface

In this section, we determine the BCs for the fields on the metascreen. To do this, we need to define the surfaces and boundaries that will be used here. Various integrations will be used over the portions of the periodic unit cell, as shown in Figs. 3(b) and 4. Volume integrals will be evaluated over regions $V_A$ and $V_B$, the volumes of the unit cell lying outside the PEC screen cross section and in $\xi_y > 0$ or $\xi_y < 0$, respectively (where $\partial A$ and $\partial B$ denote the boundaries of these regions). The normal vector $\mathbf{a}_n$ is taken "into" region $V_A$ or $V_B$ (see Fig. 4). In particular, in the aperture (denoted by $\partial A_a$ or $\partial B_a$), we have

$$\mathbf{a}_n|_{\partial A_a} = -\mathbf{a}_n|_{\partial B_a} = \mathbf{a}_y. \tag{26}$$

The contours $\partial A_p$ and $\partial B_p$ are the portions of the boundary of the PEC screen in region $A$ or $B$ (see Fig. 4). In our analysis, the normal vector ($\mathbf{a}_n$) is directed outward from $C_p$ (where $C_p = \partial A_p \cup \partial B_p$ denotes the entire surface of the screen surrounding the apertures within the period cell). The interior volume of the screen is defined by $V_p$, which is divided into portions $V_{pA}$ and $V_{pB}$ lying above and below $\xi_y = 0$, respectively.

Different BCs hold on the various parts of the boundaries of these regions. For example, the boundary-layer fields $\mathbf{e}$ and $\mathbf{h}$ decay exponentially to zero on $\partial A_\infty$ (the boundary where $\xi_y \to \infty$) and on $\partial B_\infty$ (the boundary where $\xi_y \to -\infty$). These boundary-layer fields must also satisfy periodicity conditions in $\xi_x$ and $\xi_z$. Furthermore, in the aperture $\partial A_a$ or $\partial B_a$, the total tangential $E$-field is continuous, and on the surface of the PEC screen the total tangential field is zero:

$$\mathbf{a}_n \times \mathbf{E}^{A,T}|_{\partial A_a} = -\mathbf{a}_n \times \mathbf{E}^{B,T}|_{\partial B_a} \tag{27}$$

and

$$\mathbf{a}_n \times \mathbf{E}^{A,T}|_{\partial A_p} = \mathbf{a}_n \times \mathbf{E}^{B,T}|_{\partial B_p} \equiv 0. \tag{28}$$

Our goal is to develop a set of BCs for the effective field at the $y = 0$ plane (the reference plane). The effective fields on

the surface of the screen can be evaluated by extrapolation relative to the reference plane with the use of a Taylor series. Specifically, any function of the slow variables only can be expressed in the boundary layer as

$$f(\mathbf{r}) = f(x,0,z) + \nu\xi_y \left.\frac{\partial f(x,y,z)}{\partial \hat{y}}\right|_{y=0} + O(\nu^2) \quad (29)$$

where $\hat{y} = k_0 y = \nu\xi_y$ was used. Using this Taylor series expansion of (29) and the expansion (18), condition (28) is expanded to give the following for the $E$-field on $\partial A_p$:

$$\nu^0 : \mathbf{a}_n \times \mathbf{e}^{A0}|_{\partial A_p} = -\mathbf{a}_n \times \mathbf{E}^{A0}(\mathbf{r}_o) \quad (30)$$

$$\nu^1 : \mathbf{a}_n \times \mathbf{e}^{A1}|_{\partial A_p} = -\xi_y \mathbf{a}_n \times \left[\frac{\partial}{\partial \hat{y}}\mathbf{E}^{A0}\right]_{y=0} - \mathbf{a}_n \times \mathbf{E}^{A1}(\mathbf{r}_o) \quad (31)$$

and so on. Likewise, on $\partial B_p$, we have

$$\nu^0 : \mathbf{a}_n \times \mathbf{e}^{B0}|_{\partial B_p} = -\mathbf{a}_n \times \mathbf{E}^{B0}(\mathbf{r}_o) \quad (32)$$

$$\nu^1 : \mathbf{a}_n \times \mathbf{e}^{B1}|_{\partial B_p} = -\xi_y \mathbf{a}_n \times \left[\frac{\partial}{\partial \hat{y}}\mathbf{E}^{B0}\right]_{y=0} - \mathbf{a}_n \times \mathbf{E}^{B1}(\mathbf{r}_o). \quad (33)$$

Using (18) and (27), in the aperture, we have

$$\mathbf{a}_y \times [\mathbf{e}^{Am} - \mathbf{e}^{Bm}]|_{\partial A_a/\partial B_a} = -\mathbf{a}_y \times [\mathbf{E}^{Am}(\mathbf{r}_o) - \mathbf{E}^{Bm}(\mathbf{r}_o)] \quad (34)$$

where $m$ corresponds to the different orders (i.e., 0, 1, and so on). The BC for the total tangential $H$ in the aperture is

$$\mathbf{a}_y \times [\mathbf{h}^{Am} - \mathbf{h}^{Bm}]|_{\partial A_a/\partial B_a} = -\mathbf{a}_y \times [\mathbf{H}^{Am}(\mathbf{r}_o) - \mathbf{H}^{Bm}(\mathbf{r}_o)]. \quad (35)$$

In the aperture ($\partial A_a/\partial B_a$), we also have that the normal component of the total $D$-field is continuous

$$\mathbf{a}_n \cdot \mathbf{D}^{A,T}|_{\partial A_a} = -\mathbf{a}_n \cdot \mathbf{D}^{B,T}|_{\partial B_a} \quad (36)$$

from which we get

$$\mathbf{a}_y \cdot [\mathbf{d}^{Am} - \mathbf{d}^{Bm}]|_{\partial A_a/\partial B_a} = -\mathbf{a}_y \cdot [\mathbf{D}^{Am}(\mathbf{r}_o) - \mathbf{D}^{Bm}(\mathbf{r}_o)]. \quad (37)$$

The normal component of the total $B$-field on the screen is zero, and the normal component of $B$ is continuous across the aperture. Thus, in the aperture, we have

$$\mathbf{a}_y \cdot \mathbf{B}^{A,T}|_{\partial A_a} = -\mathbf{a}_y \cdot \mathbf{B}^{B,T}|_{\partial B_a} \quad (38)$$

and on the PEC screen, we have

$$\mathbf{a}_n \cdot \mathbf{B}^{A,T}|_{\partial A_p} = \mathbf{a}_n \cdot \mathbf{B}^{B,T}|_{\partial B_p} \equiv 0. \quad (39)$$

On $\partial A_p$, this gives

$$\nu^0 : \mathbf{a}_n \cdot \mathbf{b}^{A0}|_{\partial A_p} = -\mathbf{a}_n \cdot \mathbf{B}^{A0}(\mathbf{r}_o) \quad (40)$$

$$\nu^1 : \mathbf{a}_n \cdot \mathbf{b}^{A1}|_{\partial A_p} = -\xi_y \mathbf{a}_n \cdot \left[\frac{\partial}{\partial \hat{y}}\mathbf{B}^{A0}\right]_{y=0} - \mathbf{a}_n \cdot \mathbf{B}^{A1}(\mathbf{r}_o) \quad (41)$$

and on $\partial B_p$, we have

$$\nu^0 : \mathbf{a}_n \cdot \mathbf{b}^{B0}|_{\partial B_p} = -\mathbf{a}_n \cdot \mathbf{B}^{B0}(\mathbf{r}_o) \quad (42)$$

$$\nu^1 : \mathbf{a}_n \cdot \mathbf{b}^{B1}|_{\partial B_p} = -\xi_y \mathbf{a}_n \cdot \left[\frac{\partial}{\partial \hat{y}}\mathbf{B}^{B0}\right]_{y=0} - \mathbf{a}_n \cdot \mathbf{B}^{B1}(\mathbf{r}_o) \quad (43)$$

and in the aperture, we have

$$\mathbf{a}_y \cdot [\mathbf{b}^{Am} - \mathbf{b}^{Bm}]|_{\partial A_a/\partial B_a} = -\mathbf{a}_y \cdot [\mathbf{B}^{Am}(\mathbf{r}_o) - \mathbf{B}^{Bm}(\mathbf{r}_o)]. \quad (44)$$

There are in addition *a posteriori* conditions at the surfaces of the screen. These *a posteriori* conditions relate the fields to free surface current densities or free surface charge, which we denote as $\mathbf{j}_S$ and $\rho_S$, respectively. The free surface charge is

$$\rho_S^T = \rho_S^0 + \nu\rho_S^1 + \ldots \quad (45)$$

where

$$\rho_S^m = \mathbf{a}_n \cdot [\mathbf{D}^m + \mathbf{d}^m]_{C_p} \quad (46)$$

and the free surface current density can be expanded as

$$\mathbf{j}_S^T = \mathbf{j}_S^0 + \nu\mathbf{j}_S^1 + \ldots \quad (47)$$

where

$$\mathbf{j}_S^m = \mathbf{a}_n \times [\mathbf{H}^m + \mathbf{h}^m]_{C_p}. \quad (48)$$

This last condition is the reason why we must develop an EBC on the average $E_{x,z}$ field at the $y = 0$ location and not a BC for the jump in the $H$-field at $y = 0$. Any EBCs resulting from (47) and (48) can only be used once the fields have been determined.

## III. GSTCs for a Metascreen

In this section, we derive the GSTCs for the effective fields. We begin by developing a few needed integral identities and then derive BCs for the zeroth-order effective fields at the metascreen. We then introduce normalized boundary-layer fields and state the governing equations for the zeroth-order boundary-layer fields. We show that the effective fields at the reference plane can be expressed in terms of volume and surface integrals of these zeroth-order normalized boundary-layer fields. Finally, we show that these integrals represent various surface parameters that appear explicitly in the desired GSTCs.

### A. Zeroth-Order Effective Field at the Reference Surface

Now let us look at the zeroth-order field (i.e., $m = 0$). Using the solvability condition given in (90) of Appendix A and BCs for $\mathbf{e}^0$ given in (30), (32), and (34) yields

$$\int_{\partial A_a/\partial B_a} \mathbf{a}_y \times [\mathbf{E}^{A0} - \mathbf{E}^{B0}]\, dS + \int_{C_p} \mathbf{a}_n \times \mathbf{E}^0\, dS = 0 \quad (49)$$

where we have also used the fact that $\nabla_\xi \times \mathbf{e}^0 = 0$. Recall that $\mathbf{E}^{(A,B)0}$ are independent of the fast variable and can be brought outside the integral. We define

$$\int_{\partial A_a/\partial B_a} dS = \hat{S}_a \quad (50)$$

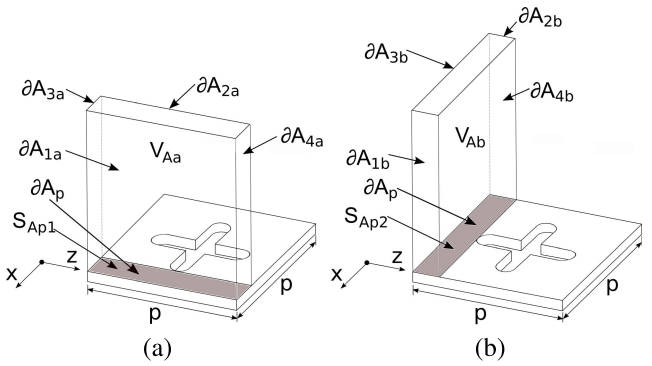


Fig. 5. Volumes and surfaces needed to for $E_x^{(0,1)}(\mathbf{r}_o)$ and $E_z^{(0,1)}(\mathbf{r}_o)$ conditions. (a) Periodic in $z$ for $E_x^{(0,1)}(\mathbf{r}_o)$. (b) Periodic in $x$ for $E_z^{(0,1)}(\mathbf{r}_o)$. A cross-shaped aperture is used for purposes of illustration.

to be the area of the aperture region intersected by $y = 0$ in scaled (fast) dimensions. We also define $\hat{S}_p$ as the surface area of the screen intersected by the plane $y = 0$ in scaled dimensions, so that $\hat{S}_p + \hat{S}_a = 1$, because the scaled area of the period cell in the plane $y = 0$ is equal to one. The actual areas in unscaled coordinates are $S_a = \hat{S}_a p^2$ and $S_p = \hat{S}_p p^2$. We can readily show that

$$\int_{\partial A_s} \mathbf{a}_n \, dS = \mathbf{a}_y \, \hat{S}_p \quad \text{and} \quad \int_{\partial B_s} \mathbf{a}_n \, dS = -\mathbf{a}_y \, \hat{S}_p. \tag{51}$$

From (49)–(51), we arrive finally at one of the desired BCs for the zeroth-order macroscopic $E$-fields

$$\mathbf{a}_y \times [\mathbf{E}^{A0}(\mathbf{r}_o) - \mathbf{E}^{B0}(\mathbf{r}_o)] = 0. \tag{52}$$

This shows that to the zeroth order, the tangential components of the effective $E$-fields are continuous across the metascreen.

Now, by enforcing the solvability conditions given in (91)–(94) of Appendix A, we obtain the two final conditions on the zeroth-order fields at the reference plane ($y = 0$). Using (21), (91), and (92), we get separate conditions from the integrals over $S_{Ap1}$ and $S_{Bp1}$ (see Appendix A and Fig. 5)

$$\mathbf{a}_x \cdot \int_{\partial A_{pa}} \mathbf{a}_n \times \mathbf{e}^{A0} \, dS = \mathbf{a}_x \cdot \int_{\partial B_{pa}} \mathbf{a}_n \times \mathbf{e}^{B0} \, dS = 0 \tag{53}$$

where $S_{Ap1}$ and $S_{Bp1}$ are the rectangular surface area of $\partial A_{pa}$ and $\partial B_{pa}$, respectively, that lie between the aperture and the $x = 0$ wall of the period cell. Note that $S_{Bp1}$ (and $\partial B_{pa}$) is equivalent to $S_{Ap1}$ (and $\partial A_{pa}$), except it corresponds to the bottom ($y < 0$) side of the screen. We are assured that these rectangles have nonzero area, because the apertures are assumed to be isolated from each other (see Fig. 5).

Proceeding as we did when deriving (52), we arrive at

$$\hat{S}_{Ap1} E_z^{A0}(\mathbf{r}_o) = 0 \quad \text{and} \quad \hat{S}_{Bp1} E_z^{B0}(\mathbf{r}_o) = 0 \tag{54}$$

where we have used the elementary results

$$\int_{\partial A_{pa}} dS = S_{Ap1} \quad \text{and} \quad \int_{\partial B_{pa}} dS = S_{Bp1}. \tag{55}$$

If $\hat{S}_{Ap1} \neq 0$ (and in turn $\hat{S}_{Bp1} \neq 0$), we have

$$E_z^{A0}(\mathbf{r}_o) = E_z^{B0}(\mathbf{r}_o) \equiv E_z^0(\mathbf{r}_o) = 0. \tag{56}$$

Following a similar procedure but now using (21), (93), and (94), we obtain:

$$E_x^{A0}(\mathbf{r}_o) = E_x^{B0}(\mathbf{r}_o) \equiv E_x^0(\mathbf{r}_o) = 0. \tag{57}$$

The two conditions given in (56) and (57) state that to the zeroth order, the macroscopic tangential $E$-fields are shorted (or forced to zero) by the PEC screen surrounding the aperture and do not penetrate through the metascreen. Any corrections to these essential BCs will appear in the first-order terms, as we will see in Section III-B.

From the $y$-component of Faraday's law, it follows that:

$$B_y^0(\mathbf{r}_0) = \frac{1}{jc}\left[ \left.\frac{\partial E_z^0(\mathbf{r})}{\partial \hat{x}}\right|_{\mathbf{r}_o} - \left.\frac{\partial E_x^0(\mathbf{r})}{\partial \hat{z}}\right|_{\mathbf{r}_o} \right] \equiv 0. \tag{58}$$

The conditions that $E_z^0(\mathbf{r}_0) = 0$ and $E_x^0(\mathbf{r}_0) = 0$ were used to obtain this expression (as well as the fact that all their tangential derivatives vanish at $y = 0$).

### *B. Analysis of the Lowest Order Boundary-Layer Fields*

With Maxwell's equations separated into the effective and boundary-layer terms (along with their BCs), we can analyze these fields separately at each higher order in $\nu$. We concentrate on the zeroth-order boundary-layer fields, because integrals of these fields are related to the surface parameters that characterize the metascreen. We have collected together the governing expressions for the zeroth-order fields $\mathbf{e}^0$ and $\mathbf{h}^0$ [governed by (21)] and their BCs, and expressed then here

$$\begin{aligned}
\nabla_\xi \cdot (\epsilon_r \mathbf{e}^0) &= 0 \Rightarrow \boldsymbol{\xi} \in V_A \quad \text{and } V_B \\
\nabla_\xi \times \mathbf{e}^0 &= 0 \Rightarrow \boldsymbol{\xi} \in V_A \quad \text{and } V_B \\
\mathbf{a}_n \times \mathbf{e}^{A0}|_{\partial A_p} &= -\mathbf{a}_n \times \mathbf{a}_y E_y^{A0}(\mathbf{r}_o) \quad \text{for } \boldsymbol{\xi} \in \partial A_p \\
\mathbf{a}_n \times \mathbf{e}^{B0}|_{\partial B_p} &= -\mathbf{a}_n \times \mathbf{a}_y E_y^{B0}(\mathbf{r}_o) \quad \text{for } \boldsymbol{\xi} \in \partial B_p \\
\mathbf{a}_y \times [\mathbf{e}^{A0} - \mathbf{e}^{B0}]|_{\partial A_a/\partial B_a} &= 0 \\
\mathbf{a}_y \cdot [\mathbf{d}^{A0} - \mathbf{d}^{B0}]|_{\partial A_a/\partial B_a} &= -\mathbf{a}_y \cdot [\mathbf{D}^{A0}(\mathbf{r}_o) - \mathbf{D}^{B0}(\mathbf{r}_o)]
\end{aligned} \tag{59}$$

and

$$\begin{aligned}
\nabla_\xi \cdot (\mu_r \mathbf{h}^0) &= 0 \Rightarrow \boldsymbol{\xi} \in S_A \quad \text{and } S_B \\
\nabla_\xi \times \mathbf{h}^0 &= 0 \Rightarrow \boldsymbol{\xi} \in S_A \quad \text{and } S_B \\
\mathbf{a}_n \cdot \mathbf{b}^{A0}|_{\partial A_p} &= -\mathbf{a}_n \cdot \mathbf{B}^{A0}(\mathbf{r}_o) \quad \text{for } \boldsymbol{\xi} \in \partial A_p \\
\mathbf{a}_n \cdot \mathbf{b}^{B0}|_{\partial B_p} &= -\mathbf{a}_n \cdot \mathbf{B}^{B0}(\mathbf{r}_o) \quad \text{for } \boldsymbol{\xi} \in \partial B_p \\
\mathbf{a}_y \cdot [\mathbf{b}^{A0} - \mathbf{b}^{B0}]|_{\partial A_a/\partial B_a} &= 0 \\
\mathbf{a}_y \times [\mathbf{h}^{A0} - \mathbf{h}^{B0}]|_{\partial A_a/\partial B_a} &= -\mathbf{a}_y \times [\mathbf{H}^{A0}(\mathbf{r}_o) - \mathbf{H}^{B0}(\mathbf{r}_o)].
\end{aligned} \tag{60}$$

As we see, the sources (forcing terms) for the boundary-layer fields contain only the macroscopic fields at the reference plane $y = 0$; as such, they will be proportional to these macroscopic fields. From (59) and (60), we can see that the sources for $\mathbf{e}^0$ are $D_y^{A0}(\mathbf{r}_o)$ and $D_y^{B0}(\mathbf{r}_o)$, and the sources for $\mathbf{h}^0$ are $H_x^{A0}(\mathbf{r}_o)$, $H_x^{B0}(\mathbf{r}_o)$, $H_z^{A0}(\mathbf{r}_o)$, and $H_z^{B0}(\mathbf{r}_o)$. By superposition then, we see that $\mathbf{e}^0$ and $\mathbf{h}^0$ must have the following forms:

$$\mathbf{e}^0 = \frac{D_y^{A0}(\mathbf{r}_o)}{\epsilon_0} \boldsymbol{\mathcal{E}}_1(\boldsymbol{\xi}) + \frac{D_y^{B0}(\mathbf{r}_o)}{\epsilon_0} \boldsymbol{\mathcal{E}}_2(\boldsymbol{\xi}) \tag{61}$$

$$\begin{aligned}
\mathbf{h}^0 = {} & H_x^{A0}(\mathbf{r}_o) \boldsymbol{\mathcal{H}}_1(\boldsymbol{\xi}) + H_x^{B0}(\mathbf{r}_o) \boldsymbol{\mathcal{H}}_2(\boldsymbol{\xi}) \\
& + H_z^{A0}(\mathbf{r}_o) \boldsymbol{\mathcal{H}}_3(\boldsymbol{\xi}) + H_z^{B0}(\mathbf{r}_o) \boldsymbol{\mathcal{H}}_4(\boldsymbol{\xi})
\end{aligned} \tag{62}$$

where $\boldsymbol{\mathcal{E}}_i$ and $\boldsymbol{\mathcal{H}}_i$ are the functions of the fast variables only, for which the governing equations are given in Appendix B. As we will see in Section III-C, these two forms for the boundary-layer fields will allow for the effective fields to appear explicitly in the GSTCs. Using the representation of $\mathbf{e}^0$ and $\mathbf{h}^0$ given in (61) and (62), we get the following for the curl of these fields:

$$\begin{aligned}\nabla_{\hat{r}} \times \mathbf{e}^0 &= -\boldsymbol{\mathcal{E}}_1 \times \nabla_{t,\hat{r}} E_y^{A0}(\mathbf{r}_o) - \boldsymbol{\mathcal{E}}_2 \times \nabla_{t,\hat{r}} E_y^{B0}(\mathbf{r}_o)\\ \nabla_{\hat{r}} \times \mathbf{h}^0 &= -\boldsymbol{\mathcal{H}}_1 \times \nabla_{t,\hat{r}} H_x^{A0}(\mathbf{r}_o) - \boldsymbol{\mathcal{H}}_2 \times \nabla_{t,\hat{r}} H_x^{B0}(\mathbf{r}_o)\\ &\quad - \boldsymbol{\mathcal{H}}_3 \times \nabla_{t,\hat{r}} H_z^{A0}(\mathbf{r}_o) - \boldsymbol{\mathcal{H}}_4 \times \nabla_{t,\hat{r}} H_z^{B0}(\mathbf{r}_o).\end{aligned} \tag{63}$$

The subscript "$t$" corresponds to derivatives with respect to $x$ and $z$ only. This is due to the fact that $\mathbf{e}$ and $\mathbf{h}$ are independent of $y$, and as a result, the curl on the left-hand side of (63) will contribute no $y$-derivatives.

### C. Boundary Conditions for the First-Order Fields and the Desired GSTCs

Here, we investigate the first-order effective fields, along with their essential BCs. This will lead to the desired GSTCs. We start by applying (90), see Appendix A, for the case $m = 1$ to obtain

$$\mathbf{a}_y \times \int_{\partial A_a} [\mathbf{e}^{A1} - \mathbf{e}^{B1}]\, dS + \int_{C_p} \mathbf{a}_n \times \mathbf{e}^1\, dS = -\int_{V_{AB}} \nabla_\xi \times \mathbf{e}^1\, dV. \tag{64}$$

From the components of Faraday's law for the macroscopic field transverse to $y$, we have

$$\mathbf{a}_y \times \frac{\partial \mathbf{E}^{\mathbf{0}}}{\partial \hat{y}}|_{\mathbf{r}_o} = -j\eta_0\mu_r\big[\mathbf{a}_x H_x^0(\mathbf{r}_o) + \mathbf{a}_z H_z^0(\mathbf{r}_o)\big] + \mathbf{a}_y \times \nabla_{t,\hat{r}} E_y^0(\mathbf{r}_0) \tag{65}$$

where $\eta_0 = \sqrt{\mu_0/\epsilon_0}$ is the free-space wave impedance. Using this and the BCs (31), (33), and (34), the left-hand side of (64) becomes

$$\begin{aligned}&-\mathbf{a}_y \times [\mathbf{E}^{A1}(\mathbf{r}_o) - \mathbf{E}^{B1}(\mathbf{r}_o)] - \hat{V}_{pA}\ \mathbf{a}_y \times \nabla_{t,\hat{r}} E_y^{A0}(\mathbf{r}_o)\\ &\quad - \hat{V}_{pB}\ \mathbf{a}_y \times \nabla_{t,\hat{r}} E_y^{B0}(\mathbf{r}_o)\\ &\quad + j\eta_0\mathbf{a}_x\big(\mu_A\ \hat{V}_{pA} H_x^{A0}(\mathbf{r}_o) + \mu_B\ \hat{V}_{pB} H_x^{B0}(\mathbf{r}_o)\big)\\ &\quad + j\eta_0\mathbf{a}_z\big(\mu_A\ \hat{V}_{pA} H_z^{A0}(\mathbf{r}_o) + \mu_B\ \hat{V}_{pB} H_z^{B0}(\mathbf{r}_o)\big)\end{aligned} \tag{66}$$

where we used the fact that

$$\int_{\partial A_p} \xi_y\, \mathbf{a}_n\, dS = \mathbf{a}_y\, \hat{V}_{pA} \ \text{ and } \ \int_{\partial B_p} \xi_y\, \mathbf{a}_n\, dS = \mathbf{a}_y\, \hat{V}_{pB} \tag{67}$$

where $\hat{V}_{pA}$ and $\hat{V}_{pB}$ are the scaled internal volumes of the screen (i.e., the plane containing the apertures) that are above and below $y = 0$, respectively (so that $\hat{V}_p = \hat{V}_{pA} + \hat{V}_{pB}$).

Using (19), (20), (22), and (61)–(63), the right-hand side (RHS) of (64) reduces to

$$\begin{aligned}&\int_{V_{AB}} \nabla_\xi \times \mathbf{e}^1\, dV\\ &= -j\eta_0 \int_{V_{AB}} \mu_r\big[H_x^{A0}(\mathbf{r}_o)\boldsymbol{\mathcal{H}}_1 + H_x^{B0}(\mathbf{r}_o)\boldsymbol{\mathcal{H}}_2\big]\, dV_\xi\\ &\quad - j\eta_0 \int_{V_{AB}} \mu_r\big[H_z^{A0}(\mathbf{r}_o)\boldsymbol{\mathcal{H}}_3 + H_z^{B0}(\mathbf{r}_o)\boldsymbol{\mathcal{H}}_4\big]\, dV_\xi\\ &\quad + \int_{V_{AB}} \boldsymbol{\mathcal{E}}_1 dV \times \nabla_{t,\hat{r}} E_y^{A0}(\mathbf{r}_o)\\ &\quad + \int_{V_{AB}} \boldsymbol{\mathcal{E}}_2 dV \times \nabla_{t,\hat{r}} E_y^{B0}(\mathbf{r}_o).\end{aligned} \tag{68}$$

Utilizing the results in [14, Appendix C], we can show that $\int \boldsymbol{\mathcal{E}}_i dV$ only has a $y$-component while $\int \boldsymbol{\mathcal{H}}_i dV$ has no $y$-components, and that

$$\begin{aligned}\int_{AB} \boldsymbol{\mathcal{E}}_1 dV_\xi &= \mathbf{a}_y\big[\alpha_{Eyy}^{AA} + \alpha_{Eyy}^{BA}\big]\\ \int_{AB} \boldsymbol{\mathcal{E}}_2 dV_\xi &= \mathbf{a}_y\big[\alpha_{Eyy}^{AB} + \alpha_{Eyy}^{BB}\big]\end{aligned} \tag{69}$$

and

$$\begin{aligned}\int_{(A,B)} \boldsymbol{\mathcal{H}}_1 dV_\xi &= \mathbf{a}_x\alpha_{Mxx}^{(A,B)A} + \mathbf{a}_z\alpha_{Mzx}^{(A,B)A}\\ \int_{(A,B)} \boldsymbol{\mathcal{H}}_2 dV_\xi &= \mathbf{a}_x\alpha_{Mxx}^{(A,B)B} + \mathbf{a}_z\alpha_{Mzx}^{(A,B)B}\\ \int_{(A,B)} \boldsymbol{\mathcal{H}}_3 dV_\xi &= \mathbf{a}_x\alpha_{Mxz}^{(A,B)A} + \mathbf{a}_z\alpha_{Mzz}^{(A,B)A}\\ \int_{(A,B)} \boldsymbol{\mathcal{H}}_4 dV_\xi &= \mathbf{a}_x\alpha_{Mxz}^{(A,B)B} + \mathbf{a}_z\alpha_{Mzz}^{(A,B)B}\end{aligned} \tag{70}$$

where $\alpha_E$ and $\alpha_M$ are defined as

$$\begin{aligned}\alpha_{Eyy}^{(A,B)[A,B]} &= \mathbf{a}_y \cdot \int_{(A,B)} \boldsymbol{\mathcal{E}}_{[1,2]} dV_\xi\\ \alpha_{Mxx}^{(A,B)[A,B]} &= \mathbf{a}_x \cdot \int_{(A,B)} \boldsymbol{\mathcal{H}}_{[1,2]} dV_\xi\\ \alpha_{Mxz}^{(A,B)[A,B]} &= \mathbf{a}_x \cdot \int_{(A,B)} \boldsymbol{\mathcal{H}}_{[3,4]} dV_\xi\\ \alpha_{Mzx}^{(A,B)[A,B]} &= \mathbf{a}_z \cdot \int_{(A,B)} \boldsymbol{\mathcal{H}}_{[1,2]} dV_\xi\\ \alpha_{Mzz}^{(A,B)[A,B]} &= \mathbf{a}_z \cdot \int_{(A,B)} \boldsymbol{\mathcal{H}}_{[3,4]} dV_\xi.\end{aligned} \tag{71}$$

The subscripts and superscripts in these various quantities have the following meanings. The first superscript ($A$ and $B$) represents an integral over either region A or region B. The second superscript implies that the source of the integrand is from either side $A$ or $B$ of the metascreen (i.e., $E_y^{A0}$ or $E_y^{B0}$ and so on). The first subscript ($E$ or $M$) corresponds to an integral of either an $\boldsymbol{\mathcal{E}}$-field or an $\boldsymbol{\mathcal{H}}$-field. The second subscript corresponds to the $x$- or $y$-component of $\boldsymbol{\alpha}_{E,M}$. The third subscript indicates the component of the excitation field that generates $\boldsymbol{\mathcal{E}}_i$ or $\boldsymbol{\mathcal{H}}_i$.

Substituting (66) and (68) into (64), the jump condition for the first-order effective $E$-field is

$$\begin{aligned}
&\mathbf{a}_y \times [\mathbf{E}^{A1}(\mathbf{r}_o) - \mathbf{E}^{B1}(\mathbf{r}_0)] \\
&\quad = -\mathbf{a}_y \times \left[ \frac{\chi_{ES}^{Ayy}}{p} \nabla_{t,\hat{r}} E_x^{A0} + \frac{\chi_{ES}^{Byy}}{p} \nabla_{t,\hat{r}} E_y^{B0}(\mathbf{r}_o) \right] \\
&\qquad - \mathbf{a}_x\, j\eta_0 \left[ \frac{\chi_{MS}^{Axx}}{p} H_x^{A0}(\mathbf{r}_o) + \frac{\chi_{MS}^{Bxx}}{p} H_x^{B0}(\mathbf{r}_o) \right. \\
&\qquad\qquad \left. + \frac{\chi_{MS}^{Axz}}{p} H_z^{A0}(\mathbf{r}_o) + \frac{\chi_{MS}^{Bxz}}{p} H_z^{B0}(\mathbf{r}_o) \right] \\
&\qquad - \mathbf{a}_z\, j\eta_0 \left[ \frac{\chi_{MS}^{Azx}}{p} H_x^{A0}(\mathbf{r}_o) + \frac{\chi_{MS}^{Bzx}}{p} H_x^{B0}(\mathbf{r}_o) \right. \\
&\qquad\qquad \left. + \frac{\chi_{MS}^{Azz}}{p} H_z^{A0}(\mathbf{r}_o) + \frac{\chi_{MS}^{Bzz}}{p} H_z^{B0}(\mathbf{r}_o) \right] \qquad (72)
\end{aligned}$$

where the coefficients $\chi_{MS}$ and $\chi_{ES}$ are interpreted as effective magnetic and electric surface susceptibilities of the metascreen, respectively, and are defined by

$$\begin{aligned}
\chi_{ES}^{Ayy} &= -p\big(\alpha_{Eyy}^{AA} + \alpha_{Eyy}^{BA} - \hat{V}_{pA}\big) \\
\chi_{ES}^{Byy} &= -p\big(\alpha_{Eyy}^{AB} + \alpha_{Eyy}^{BB} - \hat{V}_{PB}\big) \\
\chi_{MS}^{Axx} &= p\big(\mu_B \alpha_{Mxx}^{BA} + \mu_A\big[\alpha_{Mxx}^{AA} - \hat{V}_{pA}\big]\big) \\
\chi_{MS}^{Bxx} &= p\big(\mu_A \alpha_{Mxx}^{AB} + \mu_B\big[\alpha_{Mxx}^{BB} - \hat{V}_{pB}\big]\big) \\
\chi_{MS}^{(A,B)xz} &= p\big(\mu_A \alpha_{Mxz}^{A(A,B)} + \mu_B \alpha_{Mxz}^{B(A,B)}\big) \\
\chi_{MS}^{(A,B)zz} &= p\big(\mu_A \alpha_{Mzx}^{A(A,B)} + \mu_B \alpha_{Mzx}^{B(A,B)}\big) \\
\chi_{MS}^{Azz} &= p\big(\mu_B \alpha_{Mzz}^{BA} + \mu_A\big[\alpha_{Mzz}^{AA} - \hat{V}_{pA}\big]\big) \\
\chi_{MS}^{Bzz} &= p\big(\mu_A \alpha_{Mzz}^{AB} + \mu_B\big[\alpha_{Mzz}^{BB} - \hat{V}_{pB}\big]\big) \qquad (73)
\end{aligned}$$

which have units of length.

The remaining two essential BCs for the sum of $E_x^{A1} + E_x^{B1}$ and $E_z^{A1} + E_z^{B1}$ are investigated next. Using the solvability condition (91), the BC given in (22), (31), and (63), we obtain

$$\begin{aligned}
&E_z^{A1}(\mathbf{r}_o)\, S_{Ap1} \\
&= -\frac{\hat{h}}{2} S_{Ap1}\, \mathbf{a}_x \cdot \left[ \mathbf{a}_n \times \frac{\partial}{\partial \hat{y}} E_z^{A0}(\mathbf{r}_o) \right] \\
&\quad - jc\mathbf{a}_x \cdot \int \mathbf{b}^0\, dV_{Aa} + \mathbf{a}_x \cdot \left[ \int \boldsymbol{\mathcal{E}}_1\, dV_{Aa} \times \nabla_{t,\hat{r}} E_y^{A0}(\mathbf{r}_o) \right] \\
&\quad + \mathbf{a}_x \cdot \left[ \int \boldsymbol{\mathcal{E}}_2\, dV_{Aa} \times \nabla_{t,\hat{r}} E_y^{B0}(\mathbf{r}_o) \right] \qquad (74)
\end{aligned}$$

where $\hat{h}$ is the scaled thickness ($\hat{h} = h/p$) of the screen (see Fig. 4). Using (65) and (62), we get

$$\begin{aligned}
&E_z^{A1}(\mathbf{r}_o) \\
&= -j\eta_0\mu_r \left[ \mathbf{a}_x \cdot \frac{\int \boldsymbol{\mathcal{H}}_1\, dV_{Aa}}{S_{Ap1}} - \frac{\hat{h}}{2} \right] H_x^{A0} \\
&\quad - j\eta_0\mu_r \mathbf{a}_x \cdot \frac{\int \boldsymbol{\mathcal{H}}_2\, dV_{Aa}}{S_{Ap1}} H_x^{B0} - j\eta_0\mu_r \mathbf{a}_x \cdot \frac{\int \boldsymbol{\mathcal{H}}_3\, dV_{Aa}}{S_{Ap1}} H_z^{A0} \\
&\quad - j\eta_0\mu_r \mathbf{a}_x \cdot \frac{\int \boldsymbol{\mathcal{H}}_4\, dV_{Aa}}{S_{Ap1}} H_z^{B0} - \frac{\hat{h}}{2} \mathbf{a}_x \cdot \mathbf{a}_y \times \nabla E_y^{A0} \\
&\quad + \mathbf{a}_x \cdot \left[ \frac{\int \boldsymbol{\mathcal{E}}_1\, dV_{Aa}}{S_{Ap1}} \times \nabla_{t,\hat{r}} E_y^{A0} \right] \\
&\quad + \mathbf{a}_x \cdot \left[ \frac{\int \boldsymbol{\mathcal{E}}_2\, dV_{Aa}}{S_{Ap1}} \times \nabla_{t,\hat{r}} E_y^{B0} \right]. \qquad (75)
\end{aligned}$$

Using the solvability condition given is (92) and following a similar procedure as earlier, we obtain:

$$\begin{aligned}
&E_z^{B1}(\mathbf{r}_o) \\
&= +j\eta_0\mu_r \left[ \mathbf{a}_x \cdot \frac{\int \boldsymbol{\mathcal{H}}_2\, dV_{Ba}}{S_{Bp1}} - \frac{\hat{h}}{2} \right] H_x^{B0} \\
&\quad + j\eta_0\mu_r \mathbf{a}_x \cdot \frac{\int \boldsymbol{\mathcal{H}}_1\, dV_{Ba}}{S_{Bp1}} H_x^{A0} + j\eta_0\mu_r \mathbf{a}_x \cdot \frac{\int \boldsymbol{\mathcal{H}}_3\, dV_{Ba}}{S_{Bp1}} H_z^{A0} \\
&\quad + j\eta_0\mu_r \mathbf{a}_x \cdot \frac{\int \boldsymbol{\mathcal{H}}_4\, dV_{Ba}}{S_{Bp1}} H_z^{B0} + \frac{\hat{h}}{2} \mathbf{a}_x \cdot \big[\mathbf{a}_y \times \nabla E_y^{B0}\big] \\
&\quad - \mathbf{a}_x \cdot \left[ \frac{\int \boldsymbol{\mathcal{E}}_1\, dV_{Ba}}{S_{Bp1}} \times \nabla_{t,\hat{r}} E_y^{A0} \right] \\
&\quad - \mathbf{a}_x \cdot \left[ \frac{\int \boldsymbol{\mathcal{E}}_2\, dV_{Ba}}{S_{Bp1}} \times \nabla_{t,\hat{r}} E_y^{B0} \right]. \qquad (76)
\end{aligned}$$

By adding $E_z^{A1}(\mathbf{r}_o)$ and $E_z^{B1}(\mathbf{r}_o)$, we obtain

$$\begin{aligned}
&\big[E_z^{A1}(\mathbf{r}_o) + E_z^{B1}(\mathbf{r}_o)\big] \\
&\quad = -\frac{\pi_{ES}^{Ayy}}{p} \frac{\partial E_y^{A0}(\mathbf{r}_o)}{\partial \hat{z}} + \frac{\pi_{ES}^{Byy}}{p} \frac{\partial E_y^{B0}(\mathbf{r}_o)}{\partial \hat{z}} \\
&\qquad - j\eta_0 \left[ \frac{\pi_{MS}^{Axx}}{p} H_x^{A0} - \frac{\pi_{MS}^{Bxx}}{p} H_x^{B0} \right] \\
&\qquad - j\eta_0 \left[ \frac{\pi_{MS}^{Axz}}{p} H_z^{A0} - \frac{\pi_{MS}^{Bxz}}{p} H_z^{B0} \right] \qquad (77)
\end{aligned}$$

where

$$\begin{aligned}
\pi_{ES}^{(A,B)yy} &= -p \left[ \mathbf{a}_y \cdot \frac{\int \boldsymbol{\mathcal{E}}_{(1,2)}\, dV_{Aa}}{S_{Ap1}} \right. \\
&\qquad \left. - \mathbf{a}_y \cdot \frac{\int \boldsymbol{\mathcal{E}}_{(1,2)}\, dV_{Ba}}{S_{Bp1}} - \frac{\hat{h}}{2} \right] \\
\pi_{MS}^{(A,B)xx} &= p \left[ \mu_A\, \mathbf{a}_x \cdot \frac{\int \boldsymbol{\mathcal{H}}_{(1,2)}\, dV_{Aa}}{S_{Ap1}} \right. \\
&\qquad \left. - \mu_B\, \mathbf{a}_x \cdot \frac{\int \boldsymbol{\mathcal{H}}_{(1,2)}\, dV_{Ba}}{S_{Bp1}} - \frac{\hat{h}}{2} \right] \\
\pi_{MS}^{(A,B)xz} &= p \left[ \mu_A\, \mathbf{a}_x \cdot \frac{\int \boldsymbol{\mathcal{H}}_{(3,4)} dV_{Aa}}{S_{Ap1}} \right. \\
&\qquad \left. - \mu_B\, \mathbf{a}_x \cdot \frac{\int \boldsymbol{\mathcal{H}}_{(3,4)}\, dV_{Ba}}{S_{Bp1}} \right] \qquad (78)
\end{aligned}$$

and are interpreted as effective magnetic and electric surface *porosities* of the metascreen.

Using the solvability conditions (93) and (94) and following a similar procedure as ealier, we have:

$$\begin{aligned}
&\big[E_x^{A1}(\mathbf{r}_o) + E_x^{B1}(\mathbf{r}_o)\big] \\
&\quad = -\frac{\pi_{ES}^{Ayy}}{p} \frac{\partial E_y^{A0}(\mathbf{r}_o)}{\partial \hat{x}} + \frac{\pi_{ES}^{Byy}}{p} \frac{\partial E_y^{B0}(\mathbf{r}_o)}{\partial \hat{x}} \\
&\qquad + j\eta_0 \left[ \frac{\pi_{MS}^{Azx}}{p} H_x^{A0} - \frac{\pi_{MS}^{Bzx}}{p} H_x^{B0} \right] \\
&\qquad + j\eta_0 \left[ \frac{\pi_{MS}^{Azz}}{p} H_z^{A0} - \frac{\pi_{MS}^{Bzz}}{p} H_z^{B0} \right] \qquad (79)
\end{aligned}$$

where the remaining effective magnetic surface porosities are given by

$$\pi_{MS}^{(A,B)zx} = p\left[\mu_A\,\mathbf{a}_z\cdot\frac{\int\boldsymbol{\mathcal{H}}_{(1,2)}\,dV_{Aa}}{S_{Ap1}} - \mu_B\,\mathbf{a}_z\cdot\frac{\int\boldsymbol{\mathcal{H}}_{(1,2)}\,dV_{Ba}}{S_{Bp1}}\right]$$

$$\pi_{MS}^{(A,B)zz} = p\left[\mu_A\,\mathbf{a}_z\cdot\frac{\int\boldsymbol{\mathcal{H}}_{(3,4)}\,dV_{Aa}}{S_{Ap1}} - \mu_B\,\mathbf{a}_z\cdot\frac{\int\boldsymbol{\mathcal{H}}_{(3,4)}\,dV_{Ba}}{S_{Bp1}} - \frac{\hat{h}}{2}\right]. \quad (80)$$

The two BCs for the sum of the $E_x$ and $E_z$ fields [see (77) and (79)] have the same functional form as the BC needed for an arbitrarily shaped wire grating (a metagrating) [14].

We can now combine the results for the BCs on the zeroth-order and first-order fields [i.e., (72), (77), and (79)] to obtain the required BCs for the total effective fields. Utilizing (18), the BC for the total effective $E$-field at $y = 0$ to first order in $\nu$ is

$$\mathbf{a}_y\times\left[\mathbf{E}^A(\mathbf{r}_o)-\mathbf{E}^B(\mathbf{r}_o)\right] = \mathbf{a}_y\times[\mathbf{E}^{A0}(\mathbf{r}_o)-\mathbf{E}^{B0}(\mathbf{r}_o)] + \nu\,\mathbf{a}_y\times[\mathbf{E}^{A1}(\mathbf{r}_o)-\mathbf{E}^{B1}(\mathbf{r}_o)] + O(\nu^2). \quad (81)$$

From (52), the first term of the RHS of (81) is zero, and as a result, we have to first order

$$\mathbf{a}_y\times[\mathbf{E}^A(\mathbf{r}_o)-\mathbf{E}^B(\mathbf{r}_o)] = \nu\,\mathbf{a}_y\times[\mathbf{E}^{A1}(\mathbf{r}_o)-\mathbf{E}^{B1}(\mathbf{r}_o)]. \quad (82)$$

Following similar arguments, the other two BCs can be expressed as:

$$E_z^A(\mathbf{r}_o)+E_z^B(\mathbf{r}_o) = \nu\left[E_z^{A1}(\mathbf{r}_o)+E_z^{B1}(\mathbf{r}_o)\right]$$
$$E_x^A(\mathbf{r}_o)+E_x^B(\mathbf{r}_o) = \nu\left[E_x^{A1}(\mathbf{r}_o)+E_x^{B1}(\mathbf{r}_o)\right]. \quad (83)$$

Using the fact that $\nu = pk_o$, $(\partial/\partial\hat{x}) = (1/k_o)(\partial/\partial x)$, and $(\partial/\partial\hat{z}) = (1/k_o)(\partial/\partial z)$, the BC for these fields can be written in terms of the original unscaled variables as

$$\begin{aligned}\mathbf{a}_y\times[\mathbf{E}^A(\mathbf{r}_o)-\mathbf{E}^B(\mathbf{r}_0)] &= -\mathbf{a}_x\,j\omega\mu_0\left[\chi_{MS}^{Axx}H_x^A(\mathbf{r}_o)+\chi_{MS}^{Bxx}H_x^B(\mathbf{r}_o) + \chi_{MS}^{Axz}H_z^A(\mathbf{r}_o)+\chi_{MS}^{Bxz}H_z^B(\mathbf{r}_o)\right]\\ &\quad -\mathbf{a}_z\,j\omega\mu_0\left[\chi_{MS}^{Azx}H_x^A(\mathbf{r}_o)+\chi_{MS}^{Bzx}H_x^B(\mathbf{r}_o) + \chi_{MS}^{Azz}H_z^A(\mathbf{r}_o)+\chi_{MS}^{Bzz}H_z^B(\mathbf{r}_o)\right]\\ &\quad -\mathbf{a}_y\times\left[\chi_{ES}^{Ayy}\nabla_t E_y^A(\mathbf{r}_o)+\chi_{ES}^{Byy}\nabla_t E_y^B(\mathbf{r}_o)\right] \quad (84)\end{aligned}$$

for the jump in the tangential $E$-field, and

$$\begin{aligned}\mathbf{a}_y\times[\mathbf{E}^A(\mathbf{r}_o)+\mathbf{E}^B(\mathbf{r}_0)] &= -\mathbf{a}_x\,j\omega\mu_0\left[\pi_{MS}^{Axx}H_x^A(\mathbf{r}_o)-\pi_{MS}^{Bxx}H_x^B(\mathbf{r}_o) + \pi_{MS}^{Axz}H_z^A(\mathbf{r}_o)-\pi_{MS}^{Bxz}H_z^B(\mathbf{r}_o)\right]\\ &\quad -\mathbf{a}_z\,j\omega\mu_0\left[\pi_{MS}^{Azx}H_x^A(\mathbf{r}_o)-\pi_{MS}^{Bzx}H_x^B(\mathbf{r}_o) + \pi_{MS}^{Azz}H_z^A(\mathbf{r}_o)-\pi_{MS}^{Bzz}H_z^B(\mathbf{r}_o)\right]\\ &\quad -\mathbf{a}_y\times\left[\pi_{ES}^{Ayy}\nabla_t E_y^A(\mathbf{r}_o)-\pi_{ES}^{Byy}\nabla_t E_y^B(\mathbf{r}_o)\right] \quad (85)\end{aligned}$$

for the sum (twice the average) of the tangential $E$-field.

The two BCs (or the GSTCs) given in (84) and (85) are the main results of this paper. The GSTCs for the metascreen are distinctive in that they have a different form from those of a metafilm (see [13], [17]) while having some similarities to the form of the GSTCs for a wire grating [14]. The required surface parameters in the GSTCs for the metafilm are all interpreted as effective magnetic and electric surface susceptibilities ($\chi_{MS}$ and $\chi_{ES}$), while some of the surface parameters required in the GSTCs for the metascreen are interpreted as effective surface porosities ($\pi_{ES}$ and $\pi_{MS}$). The surface porosities are required because of the possibility of the metascreen shorting out the fields and allowing no penetration of the fields from one side of the screen to the other. We see that the only surface parameters that appear in (84) are surface susceptibilities. Moreover, (84) has the identical functional form as that obtained for the jump condition on **E** for a metafilm. For the metascreen, there is no essential jump condition for **H** (as was needed for the metafilm), but instead a condition (85) on the average tangential **E**, which requires the surface porosities.

Furthermore, multiple-scale homogenization accounts for spatial dispersion, but it does so in an approximate manner. In the method used in this paper, the GSTCs we have obtained do include spatial dispersion (as least to first order) through the gradient terms that appear in the BCs. For example, reflection and transmission coefficients of an incident plane wave will possess a dependence on the incidence angle because of these gradients (see [34], [35]). If the spatial dispersion (wavenumber dependence of effective parameters in the GSTC) was accounted for in a different manner by some other method and is then expanded in a power series in the wavenumber, our result is obtained as the leading-order correction.

## IV. Validity of the Formulation and the Surface Parameters

The question of the validity of the GSTCs derived has two main aspects. First is whether the functional form itself of the GSTCs is correct, and second is whether the expressions for the surface parameters expressed in terms of the static field problems as laid out in this paper yield accurate numerical results. As far as the functional form of the GSTCs given in this paper is concerned, the GSTC for the jump in the tangential field has the same form as that for a metafilm, while that for the sum of the tangential fields has the same form as that needed for a metagrating. Moreover, the GSTCs given in (84) and (85) have the same functional form as those obtained in [32] and [33] using a different approach. The GSTCs derived in [32] and [33] are limited in two ways, and thus, the ones presented here are of more general applicability. First, the analysis in [32] and [33] assumes dipole-type interactions between the apertures. As a result, Clausius–Mossotti type expressions are obtained for the surface susceptibilities and surface porosities, which assume that the apertures are not too closely spaced (an assumption that breaks down if the apertures are tightly packed). Moreover, the analysis in [32] and [33] assumes that the apertures of the metascreen have enough symmetry that the surface susceptibility dyadics and

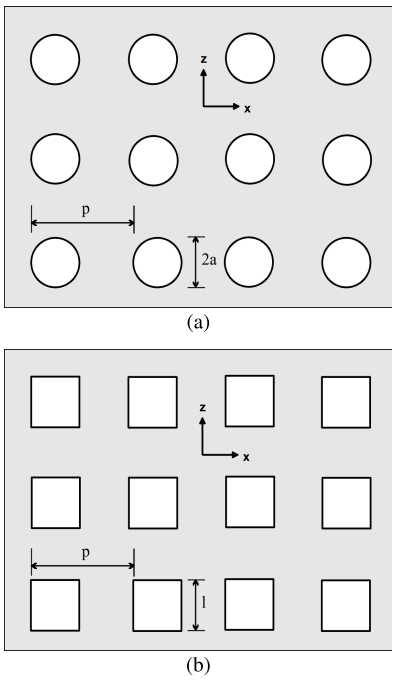


Fig. 6. Metascreen composed of (a) circular apertures and (b) square apertures. Both these metascreens have thickness $h$.

surface porosities have only diagonal terms. For arbitrarily shaped apertures, we should expect off-diagonal terms to appear in these surface parameters. In fact, we have shown that, in general, these types of off-diagonal terms are present in the GSTCs for metafilms [17] and for metagratings [14]; from (84) and (85), we see that, in general, they are also present in the GSTCs for a metascreen. Thus, while the GSTCs developed in this paper have the same functional form as those in [32] and [33], the GSTCs in this paper are more general and can be used to analyze and synthesize metascreens of very general form.

Next, we consider the validity of the expressions for the surface parameters as expressed in terms of the static fields defined in Appendix B. To determine the surface susceptibilities and surface porosities as derived in this paper, solutions of the boundary problems for the normalized boundary-layer fields given in Appendix B are required, and then, various integrals of these fields must be carried out as described in Section III-C. We used the commercial numerical modeling program COMSOL (mentioning this software is not an endorsement but is only intended to clarify what was done in this paper) to carry out this analysis for the arrays of circular and square apertures, as shown in Fig. 6. In these metascreens, we assume that the materials on both sides of the metascreen are free space and the thickness of the metascreen is $h = 10$ mm. The static fields having been determined, the integrals (71), (73), and (80) were numerically evaluated to determine $\chi_{MS}^{Azz}$ and $\pi_{MS}^{Azz}$ for both arrays. The results are shown in Figs. 7 and 8. Note that since this array is symmetric, $\chi_{MS}^{Bzz} = \chi_{MS}^{Azz}$ and $\pi_{MS}^{Bzz} = \pi_{MS}^{Azz}$.

In separate publications, we have used the GSTCs derived in this paper to derive the transmission and reflection coefficients for a plane-wave incident onto a metascreen [34], [35]. From the expressions for these coefficients (determined either from

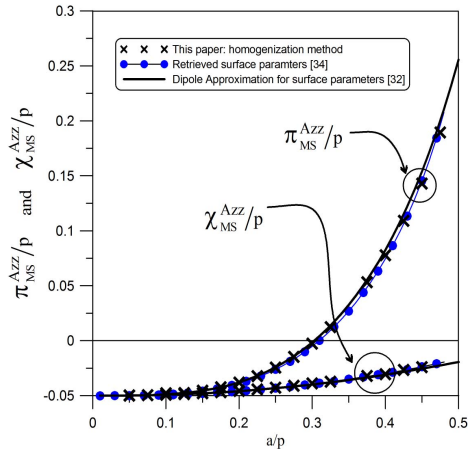


Fig. 7. Magnetic surface susceptibility and surface porosity for an array of circular apertures: $p = 100$ mm and $h = 10$ mm.

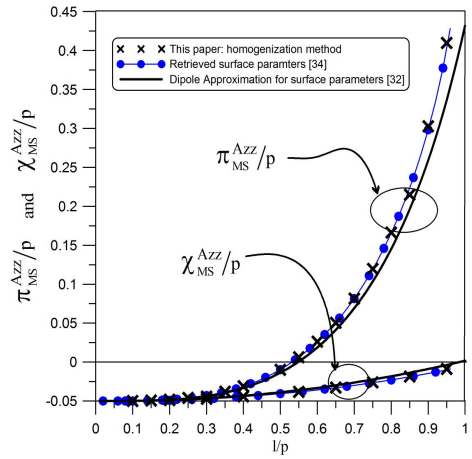


Fig. 8. Magnetic surface susceptibility and surface porosity for an array of square apertures: $p = 100$ mm and $h = 10$ mm.

numerical simulations or measurements), we have derived a retrieval technique for obtaining the surface susceptibilities and surface porosities [34]. The retrieved values for $\chi_{MS}^{Azz}$ and $\pi_{MS}^{Azz}$ obtained from the method of [34] are also shown in Figs. 7 and 8. Moreover, closed-form expressions for the surface porosities and susceptibilities were obtained in [32] using dipole-interaction approximations for arrays of circular or square apertures. Results of these approximations are also shown in Figs. 7 and 8. From the comparisons shown in Figs. 7 and 8, we see that the results obtained using the surface susceptibilities and porosities given in this paper compare very well with those obtained from the retrieval method given in [34] and a little less so (especially when the aperture size becomes comparable to the period) with those from the dipole approximation (illustrating some of the limitations in the dipole approximations and indicating that the surface parameters are better determined either from the homogenization-based approach or from the retrieval approach). These results validate the homogenization-based formulation for the surface parameters and help validate the GSTCs in general.

## V. Conclusion and Discussion

The interaction of electromagnetic fields with a metascreen embedded in a material interface is investigated here, where

we have demonstrated, now, a homogenization method which can be used to derive GSTCs for the macroscopic electromagnetic fields at the surface of a metascreen. The surface parameters in these BCs are interpreted as effective magnetic and electric surface susceptibilities and surface porosities, which are related to the geometry of the apertures that constitute the metascreen. The effective surface parameters (the effective magnetic and electric surface porosities and surface susceptibilities) are uniquely defined and, as such, represent the physical quantities that uniquely characterize the metascreen. The homogenization-based formulation for the surface parameters was validated by comparing results for the surface susceptibility and surface porosity of two different arrays with those obtained from a retrieval approach and from a dipole approximation.

The GSTCs required for the metascreen are interesting in that the essential BC for the jump in the tangential $E$-field is identical in form to that required for a metafilm. However, unlike the metafilm, there is no essential BC for the jump in the tangential $H$-fields, and in place of this, we have essential BCs for the sum of the tangential $E$-fields. For the metascreen, BCs for the jump in the $H$-fields are *a posteriori* BCs and can only be used once the fields have been solved for, using the essential BCs. As such, the GSTCs for the metascreen have some similar characteristics to those seen in metagrating [14].

The surface parameters that uniquely characterize the metascreen are related to the geometry of the apertures that constitute the metascreen, and can exhibit anisotropic properties if this geometry is sufficiently asymmetric. These anisotropic properties can result in conversion between TE and TM polarizations when a plane wave is incident onto a metascreen. These GSTCs are used in [35] to derive the plane-wave transmission and reflection coefficients of an anisotropic metascreen and illustrate this cross polarization.

Using the homogenization method, we have presented the details for calculating the required surface susceptibilities and surface porosities, which require a solution of a set of static field problems. However, the GSTCs presented in this paper can be used to determine (or retrieve) these surface parameters from computed or measured transmission and reflection data. This type of retrieval is analogous to what was done for characterizing metamaterials, metasurfaces, metafilms, and metagratings in [8], [14]–[16], [25], and [31], respectively. Indeed, in [15] and [16], the GSTCs for metafilms were used to develop retrieval algorithms for the surface susceptibilities of a metafilm. Similarly, the GSTCs presented in this paper can be used to develop retrieval algorithms for the surface porosities of a metascreen [34].

We should note, in conclusion, that to obtain a homogenization model for a more general, non-PEC screen, we would need an additional set of expressions similar to those presented in (2) and (3) for the fields inside the screen material, but an analysis similar to that carried out in this paper should allow the GSTCs to be derived. This analysis will form the topic of a future paper.

## APPENDIX

### *A. Integral Constraints (Solvability Conditions) for the Boundary-Layer Fields*

By applying Stokes' theorem to the curl of $\mathbf{e}^m$ by integrating it over the volume $V_A$ shown in Figs. 3(b) and 4, we obtain

$$\int_{V_A} \nabla_\xi \times \mathbf{e}^m dV_A = -\oint_{\partial V_A} \mathbf{a}_n \times \mathbf{e}^m \, dS \tag{86}$$

and the integral over the boundary of $V_A$ breaks up into

$$\oint_{\partial V_A} = \int_{\partial A_a} + \int_{\partial A_p} + \int_{\xi_y \to -\infty} + \sum_{n=1}^{4} \int_{\partial A_n} \tag{87}$$

where $\partial A_n$ corresponds to the four vertical sides of $V_A$. Because the fields are periodic, the integrals over these four sides ($\sum \int_{\partial A_n}$) sum to zero. Also, because $\mathbf{e}^m \to 0$ as $|\xi_y| \to \infty$, the third term in (87) vanishes. Thus, (86) reduces to

$$\mathbf{a}_y \times \int_{\partial A_a} \mathbf{e}^{Am} dS + \int_{\partial A_p} \mathbf{a}_n \times \mathbf{e}^{Am} dS = -\int_{V_A} \nabla_\xi \times \mathbf{e}^m \, dV_A. \tag{88}$$

Similarly, by integrating $\nabla_\xi \times \mathbf{e}^m$ over the volume $V_B$ as shown in Figs. 3(b) and 4 (a noting directions of the surface normals $\mathbf{a}_n$), we have

$$-\mathbf{a}_y \times \int_{\partial B_a} \mathbf{e}^{Bm} \, dS + \int_{\partial B_p} \mathbf{a}_n \times \mathbf{e}^{Bm} \, dS = -\int_{V_B} \nabla_\xi \times \mathbf{e}^m \, dV_B \tag{89}$$

where we use the fact that $\mathbf{a}_n = -\mathbf{a}_y$ on $\partial B_a$. By adding (89) to (88), we obtain

$$\mathbf{a}_y \times \int_{\partial A_a} \left[\mathbf{e}^{Am} - \mathbf{e}^{Bm}\right] dS + \int_{C_p} \mathbf{a}_n \times \mathbf{e}^m \, dS = -\int_{V_{AB}} \nabla_\xi \times \mathbf{e}^m \, dV. \tag{90}$$

where $V_{AB}$ denotes the union of volumes $V_A$ and $V_B$.

Two final constraints on the zeroth-order fields at $y = 0$ can be obtained by enforcing conditions over different regions than those used earlier. To accomplish this, we carry out the integration of the fast curl of $\mathbf{e}^m$ only over those portions $V_{Aa}$ and $V_{Ba}$ of them that lie directly above and below the section of screen corresponding to the region shown in Fig. 5(a). Contributions from $\partial A_{3a}$ and $\partial A_{4a}$ cancel due to periodicity. The contributions from the sides $\partial A_{1a}$ and $\partial A_{a2}$ (or $\partial B_{a1}$ and $\partial B_{a2}$ for an integral over the same region for $y < 0$) no longer cancel by periodicity as they did before. However, if we take only the $x$-components of the resulting equations, these side contributions will vanish, because $\mathbf{a}_n = \pm \mathbf{a}_x$ there, giving

$$\mathbf{a}_x \cdot \int \nabla \times \mathbf{e}^m \, dV_{Aa} = -\mathbf{a}_x \cdot \int_{\partial A_{pa}} \mathbf{a}_n \times \mathbf{e}^m \, dS \tag{91}$$

and for the bottom ($y < 0$) side of the plane

$$\mathbf{a}_x \cdot \int \nabla \times \mathbf{e}^m \, dV_{Ba} = -\mathbf{a}_x \cdot \int_{\partial B_{pa}} \mathbf{a}_n \times \mathbf{e}^m \, dS. \tag{92}$$

Similarly, carrying out the integration only over those portions $V_{Ab}$ and $V_{Bb}$ of $V_A$ and $V_B$ that lie directly above and

below the section of screen corresponding to the region shown in Fig. 5(b), we obtain

$$\mathbf{a}_z \cdot \int \nabla \times \mathbf{e}^m \, dV_{Ab} = -\mathbf{a}_z \cdot \int_{\partial A_{pb}} \mathbf{a}_n \times \mathbf{e}^m \, dS \qquad (93)$$

and for the bottom ($y < 0$) side of the plane

$$\mathbf{a}_z \cdot \int \nabla \times \mathbf{e}^m \, dV_{Bb} = -\mathbf{a}_z \cdot \int_{\partial B_{pb}} \mathbf{a}_n \times \mathbf{e}^m \, dS. \qquad (94)$$

### *B. Normalized Boundary-Layer Fields*

From (59) and (61), $\boldsymbol{\mathcal{E}}_i$ are shown to obey

$$\begin{aligned}
\nabla_\xi \times \boldsymbol{\mathcal{E}}_i &= 0 \Rightarrow \boldsymbol{\xi} \in V_A \quad \text{and } V_B \\
\nabla_\xi \cdot (\epsilon_r \boldsymbol{\mathcal{E}}_i) &= 0 \Rightarrow \boldsymbol{\xi} \in V_A \quad \text{and } V_B \\
\mathbf{a}_n \times \boldsymbol{\mathcal{E}}_i^A\big|_{\partial A_p} &= -A_i \mathbf{a}_n \times \mathbf{a}_y|_{\partial A_p} \\
\mathbf{a}_n \times \boldsymbol{\mathcal{E}}_i^B\big|_{\partial B_p} &= -B_i \mathbf{a}_n \times \mathbf{a}_y|_{\partial B_p} \\
\mathbf{a}_y \cdot \left[\epsilon_r^A \boldsymbol{\mathcal{E}}_i^A - \epsilon_r^B \boldsymbol{\mathcal{E}}_i^B\right]\big|_{\partial A_a/\partial B_a} &= V_i \\
\mathbf{a}_y \times \left[\boldsymbol{\mathcal{E}}_i^A - \boldsymbol{\mathcal{E}}_i^B\right]\big|_{\partial A_a/\partial B_a} &= 0 \\
\oint_{C_s} \mathbf{a}_n \cdot (\epsilon_0 \boldsymbol{\mathcal{E}}_i) \, dS_\xi &= 0
\end{aligned} \qquad (95)$$

where the sources for $\boldsymbol{\mathcal{E}}_1$ and $\boldsymbol{\mathcal{E}}_2$ (that appear in the third, fourth, and fifth lines of these expressions) are given by

$$\begin{aligned}
A_1 = 1 \quad &\text{and } B_1 = 0 \\
A_2 = 0 \quad &\text{and } \mathrm{B}_2 = 1 \\
V_1 = -1 \quad &\text{and } \mathrm{V}_2 = 1
\end{aligned} \qquad (96)$$

respectively. Similarly, from (62) and (60), $\boldsymbol{\mathcal{H}}_i$ are shown to obey

$$\begin{aligned}
\nabla_\xi \times \boldsymbol{\mathcal{H}}_i &= 0 \Rightarrow \boldsymbol{\xi} \in V_A \quad \text{and } V_B \\
\nabla_\xi \cdot (\mu_r \boldsymbol{\mathcal{H}}_i) &= 0 \Rightarrow \boldsymbol{\xi} \in V_A \quad \text{and } V_B \\
\mathbf{a}_n \cdot \left(\mu_r^A \boldsymbol{\mathcal{H}}_i\right)\big|_{\partial A_p} &= -C_i \mathbf{a}_n \cdot \mathbf{a}_i|_{\partial A_p} \\
\mathbf{a}_n \cdot \left(\mu_r^B \boldsymbol{\mathcal{H}}_i\right)\big|_{\partial B_p} &= -D_i \mathbf{a}_n \cdot \mathbf{a}_i|_{\partial B_p} \\
\mathbf{a}_y \times \left[\boldsymbol{\mathcal{H}}_i^A - \boldsymbol{\mathcal{H}}_i^B\right]\big|_{\partial A_a/\partial B_a} &= \mathbf{a}_y \times \mathbf{a}_i \; W_i \\
\mathbf{a}_y \cdot \left[\mu_r^A \boldsymbol{\mathcal{H}}_i^A - \mu_r^B \boldsymbol{\mathcal{H}}_i^B\right]\big|_{\partial A_a/\partial B_a} &= 0 \\
\oint_{C_s} \mathbf{a}_n \times \boldsymbol{\mathcal{H}}_i, \, dS_\xi &= 0
\end{aligned} \qquad (97)$$

where the sources for $\boldsymbol{\mathcal{H}}_1$, $\boldsymbol{\mathcal{H}}_2$, $\boldsymbol{\mathcal{H}}_3$, and $\boldsymbol{\mathcal{H}}_4$ are given by

$$\begin{aligned}
&\mathbf{a}_1 = \mathbf{a}_x \quad C_1 = 1 \quad \text{and } D_1 = 0 \\
&\mathbf{a}_2 = \mathbf{a}_x \quad C_2 = 0 \quad \text{and } D_2 = 1 \\
&\mathbf{a}_3 = \mathbf{a}_z \quad C_3 = 1 \quad \text{and } D_3 = 0 \\
&\mathbf{a}_4 = \mathbf{a}_z \quad C_4 = 0 \quad \text{and } D_3 = 1 \\
&W_1 = -1, \quad W_2 = 1, \; W_3 = -1, \; W_4 = 1
\end{aligned} \qquad (98)$$

respectively. In this set of static field problems, it is important to note that, in general, $\boldsymbol{\mathcal{E}}_i$ and $\boldsymbol{\mathcal{H}}_i$ are nonzero in both volumes (i.e., regions A and B). The fields in the two regions are coupled together by the BC in the aperture [i.e., the fifth lines in (95) and (97)].

## REFERENCES


[1] S. Zouhdi, A. Sihvola, and M. Arsalane, Eds., *Advances in Electromagnetics of Complex Media and Metamaterials*. Boston, MA, USA: Kluwer, 2002.

[2] C. Caloz and T. Itoh, *Electromagnetic Metamaterials: Transmission Line Theory and Microwave Applications*. Hoboken, NJ, USA: IEEE Press, 2005.

[3] G. V. Eleftheriades and K. G. Balmain, *Negative-Refraction Metamaterials: Fundamental Principles and Applications*. Hoboken, NJ, USA: IEEE Press, 2005.

[4] N. Engheta and R. W. Ziolkowski, *Electromagnetic Metamaterials: Physics and Engineering Explorations*. Piscataway, NJ, USA: IEEE Press, 2006.

[5] R. Marqués, F. Martín, and M. Sorolla, *Metamaterials With Negative Parameters: Theory, Design, and Microwave Applications*. Hoboken, NJ, USA: Wiley, 2008.

[6] F. Capolino, Ed., *Metamaterials Handbook: Theory Phenomena Metamaterials*. Boca Raton, FL, USA: CRC Press, 2009.

[7] T. J. Cui, D. R. Smith, and R. Liu, Eds., *Metamaterials: Theory, Design, and Applications*. New York, NY, USA: Springer, 2010.

[8] C. L. Holloway, E. F. Kuester, J. A. Gordon, J. O'Hara, J. Booth, and D. R. Smith, "An overview of the theory and applications of metasurfaces: The two-dimensional equivalents of metamaterials," *IEEE Antennas Propag. Mag.*, vol. 54, no. 2, pp. 10–35, Apr. 2012.

[9] A. A. Maradudin, Ed., *Structured Surfaces as Optical Metamaterials*. Cambridge, U.K.: Cambridge Univ. Press, 2011.

[10] T. K. Wu, *Frequency Selective Surface and Grid Array*. New York, NY, USA: Wiley, 1995.

[11] B. A. Munk, *Frequency Selective Surfaces: Theory and Design*. New York, NY, USA: Wiley, 2000.

[12] C. L. Holloway, D. C. Love, E. F. Kuester, J. A. Gordon, and D. A. Hill, "Use of generalized sheet transition conditions to model guided waves on metasurfaces/metafilms," *IEEE Trans. Antennas Propag.*, vol. 60, no. 11, pp. 5173–5186, Nov. 2012.

[13] E. F. Kuester, M. A. Mohamed, M. Piket-May, and C. L. Holloway, "Averaged transition conditions for electromagnetic fields at a metafilm," *IEEE Trans. Antennas Propag.*, vol. 51, no. 10, pp. 2641–2651, Oct. 2003.

[14] C. L. Holloway, E. F. Kuester, and A. Dienstfrey, "A homogenization technique for obtaining generalized sheet transition conditions for an arbitrarily shaped coated wire grating," *Radio Sci.*, vol. 49, no. 10, pp. 813–850, Oct. 2014.

[15] C. L. Holloway, A. Dienstfrey, E. F. Kuester, J. F. O'Hara, A. K. Azad, and A. J. Taylor, "A discussion on the interpretation and characterization of metafilms/metasurfaces: The two-dimensional equivalent of metamaterials," *Metamaterials*, vol. 3, no. 2, pp. 100–112, 2009.

[16] C. L. Holloway, E. F. Kuester, and A. Dienstfrey, "Characterizing metasurfaces/metafilms: The connection between surface susceptibilities and effective material properties," *IEEE Antennas Wireless Propag. Lett.*, vol. 10, pp. 1507–1511, 2011.

[17] C. L. Holloway and E. F. Kuester, "A homogenization technique for obtaining generalized sheet-transition conditions for a metafilm embedded in a magnetodielectric interface," *IEEE Trans. Antennas Propag.*, vol. 64, no. 11, pp. 4671–4686, Nov. 2016.

[18] E. Sanchez-Palencia, "Comportements local et macroscopique d'un type de milieux physiques hétérogenes," *Int. J. Eng. Sci.*, vol. 12, no. 4, pp. 331–351, 1974.

[19] E. F. Kuester and C. L. Holloway, "A low-frequency model for wedge or pyramid absorber arrays—I: Theory," *IEEE Trans. Electromag. Compat.*, vol. 36, no. 4, pp. 300–306, Nov. 1994.

[20] E. Sanchez-Palencia, *Non-Homogeneous Media and Vibration Theory* (Lecture Notes in Physics). Berlin, Germany: Springer-Verlag, 1980, pp. 68–77.

[21] A. Bensoussan, J.-L. Lions, and G. Papanicolaou, *Asymptotic Analysis for Periodic Structures*. Amsterdam, The Netherlands: North Holland, 1978.

[22] N. S. Bakhvalov and G. Panasenko, *Homogenisation: Averaging Processes in Periodic Media*. Dordecht, The Netherlands: Kluwer, 1989.

[23] C. L. Holloway and E. F. Kuester, "Impedance-type boundary conditions for a periodic interface between a dielectric and a highly conducting medium," *IEEE Trans. Antennas Propag.*, vol. 48, no. 10, pp. 1660–1672, Oct. 2000.

[24] C. L. Holloway and E. F. Kuester, "Equivalent boundary conditions for a perfectly conducting periodic surface with a cover layer," *Radio Sci.*, vol. 35, no. 3, pp. 661–681, 2000.

[25] C. L. Holloway and E. F. Kuester, "Corrections to the classical continuity boundary conditions at the interface of a composite medium," *Photon. Nanostruct. Fundam. Appl.*, vol. 11, no. 4, pp. 397–422, 2013.
[26] G. Bouchitté and D. Felbacq, "Homogenization near resonances and artificial magnetism from dielectrics," *Comptes Rendus Math.*, vol. 339, no. 5, pp. 377–382, 2004.
[27] G. Bouchitté, C. Bourel, and D. Felbacq, "Homogenization of the 3D Maxwell system near resonances and artificial magnetism," *Comptes Rendus Math.*, vol. 347, pp. 571–576, May 2009.
[28] D. Felbacq, B. Guizal, G. Bouchitté, and C. Bourel, "Resonant homogenization of a dielectric metamaterial," *Microw. Opt. Technol. Lett.*, vol. 51, no. 11, pp. 2695–2701, 2009.
[29] G. Bouchitté and B. Schweizer, "Homogenization of Maxwell's equations in a split ring geometry," *Multiscale Model. Simul.*, vol. 8, no. 3, pp. 717–750, 2010.
[30] L. A. Wainstein, "On the electrodynamic theory of grids," in *High-Power Electronics*, (in Russian), P. L. Kapitza and L. A. Wainstein, Eds. Oxford, U.K.: Pergamon, 1966, ch. 2, pp. 14–48.
[31] T. B. A. Senior and J. L. Volakis, *Approximate Boundary Conditions in Electromagnetics*. London, U.K.: IEE, 1995, p. 163.
[32] E.F. Kuester and E. Liu, "Average transition conditions for electromagnetic fields at a metascreen of nonzero thickness," 2018.
[33] E. F. Kuester, E. Liu, and N. J. Krull, "Average transition conditions for electromagnetic fields at a metascreen of vanishing thickness," 2018.
[34] C. L. Holloway and E. F. Kuester, "Reflection and transmission coefficients for a metascreen: Retrieval approach for determining effective surface-susceptibilities and surface-porosities," *IEEE Trans. Antennas Propag.*, to be published.
[35] C. L. Holloway and E. F. Kuester, "Reflection and transmission coefficients for an anisotropic metascreen: Conversion between TE and TM modes," *Phys. Rev. B, Condens. Matter*, to be published.

**Christopher L. Holloway** (S'86–M'92–SM'04–F'10) received the B.S. degree from The University of Tennessee at Chattanooga, Chattanooga, TN, USA, and the M.S. and Ph.D. degrees in electrical engineering from the University of Colorado at Boulder, Boulder, CO, USA.

In 1992, he was a Research Scientist with Electro Magnetic Applications, Inc., Lakewood, CO, USA, where he was involved in theoretical analysis and finite-difference time-domain modeling of various electromagnetic problems. From 1992 to 1994, he was with the National Center for Atmospheric Research, Boulder, CO, USA, where he was involved in wave propagation modeling, signal processing studies, and radar systems design. From 1994 to 2000, he was with the U.S. Department of Commerce, Institute for Telecommunication Sciences, Boulder, CO, USA, where he was involved in wave propagation studies. Since 2000, he has been with the National Institute of Standards and Technology, Boulder, CO, USA, where he has been involved in electromagnetic theory. He is currently with the Graduate Faculty, University of Colorado at Boulder. His current research interests include electromagnetic field theory, wave propagation, guided wave structures, remote sensing, numerical methods, metamaterials, measurement techniques, EMC/EMI issues, and atom-based metrology.

Dr. Holloway is a member of International Union of Radio Science (URSI) Commissions A, B, and E. He served as the Chair for the U.S. Commission A of the URSI from 2012 to 2015. He was the Chairman for the Technical Committee on Computational Electromagnetics (TC-9) of the IEEE Electromagnetic Compatibility Society from 2000 to 2005. He served as the Co-Chair of the Technical Committee on Nano-Technology and Advanced Materials (TC-11) of the IEEE EMC Society from 2006 to 2011. He served as an IEEE Distinguished Lecturer of the EMC Society from 2004 to 2006. He is currently an Associate Editor of the IEEE TRANSACTIONS ON ELECTROMAGNETIC COMPATIBILITY.

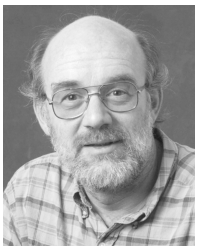

**Edward F. Kuester** (S'73–M'76–SM'95–F'98–LF'17) received the B.S. degree from Michigan State University, East Lansing, MI, USA, in 1971, and the M.S. and Ph.D. degrees from the University of Colorado at Boulder, Boulder, CO, USA, in 1974 and 1976, respectively, all in electrical engineering.

Since 1976, he has been with the Department of Electrical, Computer and Energy Engineering, University of Colorado at Boulder, where he is currently a Professor Emeritus. In 1979, he was a Summer Faculty Fellow with the Jet Propulsion Laboratory, Pasadena, CA, USA. From 1981 to 1982, he was a Visiting Professor with the Technische Hogeschool, Delft, The Netherlands. In 1992 and 1993, he was an Invited Professor with the École Polytechnique Fédérale de Lausanne, Lausanne, Switzerland. He was a Visiting Scientist with the National Institute of Standards and Technology, Boulder, CO, USA, in 2002, 2004, and 2006. He has co-authored two books, has authored chapters in two others, and has translated two books from the Russian. He has authored or co-authored over 100 papers in refereed technical journals. He is a co-holder of two U.S. patents. His current research interests include the modeling of electromagnetic phenomena of guiding and radiating structures, applied mathematics, and applied physics.

Dr. Kuester is a member of the Society for Industrial and Applied Mathematics and Commissions B and D of the International Union of Radio Science.